ELIMINATION OF NOISE FROM CURRENT MEASUREMENTS ON PULSED DISCHARGE DEVICES

by

SIDNEY SYLVESTER MEDLEY

B.Sc., University of British Columbia, 1963

A THESIS SUBMITTED IN PARTIAL FULFILMENT OF

THE REQUIREMENTS FOR THE DEGREE OF

MASTER OF SCIENCE

in the department

of

PHYSICS

We accept this thesis as conforming to the

required standard

THE UNIVERSITY OF BRITISH COLUMBIA

September, 1964

In presenting this thesis in partial fulfilment of the requirements for an advanced degree at the University of British Columbia, I agree that the Library shall make it freely available for reference and study. I further agree that permission for extensive copying of this thesis for scholarly purposes may be granted by the Head of my Department or by his representatives. It is understood that copying or publication of this thesis for financial gain shall not be allowed without my written permission.

Department of Physics

The University of British Columbia,
Vancouver 8, Canada

Date Sept. 16/64

ABSTRACT

A Rogowski coil has been used to measure current in a pulsed discharge circuit. The frequency response of the coil has been determined experimentally.

It has been established that the noise signal associated with the measurement of a pulsed discharge current is due principally to the electromagnetic radiation from the spark gap switches required in such a circuit. The radiation can be reduced by pressurizing the spark gap with argon, but at the same time the breakdown potential of the switch becomes erratic.

A simple measuring system has been devised which completely eliminates the noise signal from the current waveform. The system consists of a balanced differential preamplifier which is fed by a completely balanced measuring circuit into which a 0.5 μsec delay line has been incorporated.

ACKNOWLEDGEMENTS

I wish to thank Dr. F. L. Curzon for the excellent supervision I received while carrying out this investigation.

I am indebted to my colleague C. C. Daughney for making available to me parts of his thesis concerned with the description of the apparatus as well as for many helpful discussions.

The assistance of Mr. J. H. Turner and Mr. W. Ratzlaff in the field of electronics and the assistance of Mr. T. Knopp, Mr. J. Lees and other members of the technical staff in the construction of the apparatus is gratefully acknowledged.

I also wish to thank the National Research Council of Canada for financial assistance during the course of this work.

TABLE OF CONTENTS

APPENDICES

LIST OF ILLUSTRATIONS

Figure

1.0 INTRODUCTION

A linear Z-pinch device is an apparatus for producing a highly ionized gas or plasma. The Z-pinch device described in this thesis is readily constructed using only modest workshop facilities and is operationally rugged.

The essential part of a linear Z-pinch device is called the "discharge vessel". The discharge vessel is simply a cylinder of some nonconducting material (pyrex, for example) with an electrode fitted into each end of the cylinder. Discharging a condenser through the gas column inside the discharge vessel produces an axial current (I) and an azimuthal magnetic field ($\underline{B}$) as shown in figure 1.

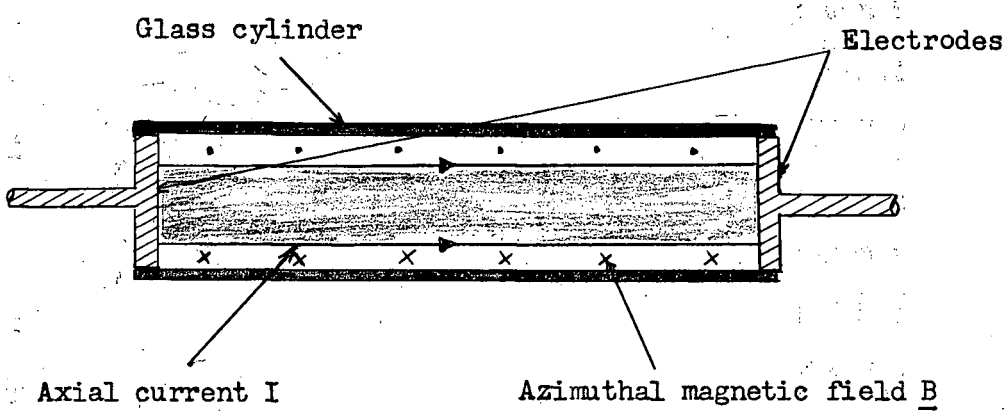

Figure 1: Schematic Diagram of Discharge Vessel

The current carrying electrons have an axial drift velocity $\underline{v}$ and experience a Lorentz force $q\ (\underline{v} \times \underline{B})$ acting radially inward. As the discharge current rises, and consequently the azimuthal magnetic field increases, the electron stream contracts radially drawing the ions in

with it by means of space charge fields. When the gas column reaches its minimum diameter it is said to be "pinched". The axial current and associated azimuthal magnetic field serve to confine the gas column and to heat the gas column by ohmic, adiabatic and shock heating.

The discharge current (I) is monitored by means of a Rogowski coil (see page 20) and an oscilloscope. However, the initial time and rate of rise of the current waveform obtained with the coil cannot be determined accurately because an electrical noise signal coincides with the initial rise of the waveform.

The investigation presented in this thesis is concerned with two problems. The first problem is to discover whether the noise signal mentioned above is a genuine noise signal or a spurious noise signal. The term "genuine noise signal" refers to a signal which is the result of voltages induced in the Rogowski coil by fluctuations in the discharge current. The term "spurious noise signal" refers to signals which enter the measuring system by way of stray coupling between the measuring and discharge circuits. The second task is to locate the sources of the noise signal in question and to eliminate them, or, if this is not possible, to minimize their influence on the measuring circuit.

Noise signals are present on all current and voltage waveforms taken in linear Z-pinch experiments but only two papers have been found which attempt to explain the source of noise. Bodin, Newton and Peacock (1960) state that the electronic noise is due to cable reflections. Curzon and Daughney (1963) suggest that an important source of noise is the spark gap switch of the discharge circuit.

The present investigation has established that the noise signal

accompanying the current waveform obtained with a Rogowski coil is due to stray coupling between the measuring and discharge circuits. Clean current waveforms are obtained by a) using a balanced measuring system and b) delaying the signal from the Rogowski coil for 0.5 μ sec before displaying it on the oscilloscope.

Also, the spark gap switch in the discharge circuit was found to be the principal source of noise. The amplitude of the noise signal produced by this switch is greatly reduced by operating the spark gap switch in an argon atmosphere.

2.0 APPARATUS

Two general considerations govern the basic design of the apparatus; first, the coaxial construction of all components, and second, the complete isolation of the high voltage discharge circuit from the low voltage triggering circuit. The purpose of coaxial construction is to minimize the magnetic field produced by the apparatus. By using coaxial construction, the current paths are arranged so as to produce only magnetic quadrupole radiation which falls off rapidly with distance. The technique of coaxial construction is well known and requires no further comment.

The purpose of the complete isolation mentioned above is twofold. First, and most important, the possibility of noise signals being produced by currents flowing from the discharge circuit to ground through the triggering electronics is eliminated and second, the operator is protected from the large currents associated with the discharge circuit. The method by which this complete isolation is achieved requires further explanation.

A block diagram of the triggering system is shown in figure 2, page 5. The thyratron trigger unit (A) supplies the initial trigger pulse. The trigger generator (B) accepts this pulse and provides a stronger output pulse which is used to trigger the spark gap switch (C) of the discharge circuit. When the switch (C) is closed, the capacitor bank (D) discharges through the discharge vessel (E).

In addition to increasing the strength of the trigger pulse, the trigger generator (B) provides complete electrical isolation between the trigger unit (A) and the discharge circuit (C, D, E). This property is

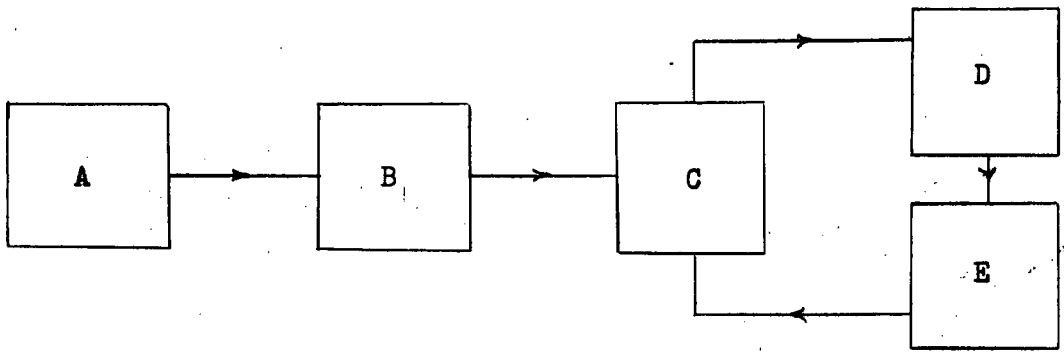

Figure 2: Block Diagram of Trigger System

A, Thyratron trigger unit; B, Trigger generator; C, Three electrode spark gap switch; D, Capacitor bank; E, Discharge vessel.

discussed in detail in subsection 2.2, page 9.

A more detailed circuit diagram of the triggering system and discharge circuit is given in figure 3, page 6. Both the trigger capacitance (C_2) and the bank capacitance (C_3) are charged to 12 kV by means of the power supply (F). The apparatus is then discharged by manually triggering the thyratron unit (A) which creates a trigger spark (T_1) in the trigger generator (B). The trigger spark (T_1) causes breakdown of the open air spark gap switch (S_1) and thus causes the capacitance (C_2) to discharge through the resistance (R_{T2}). The voltage created across the resistance (R_{T2}) is used, in turn, to create a second trigger spark (T_2) in the open air spark gap switch (S_2) of the main discharge circuit (C) and this initiates breakdown of the switch. As a result, the capacitance (C_3) discharges through the discharge vessel (E).

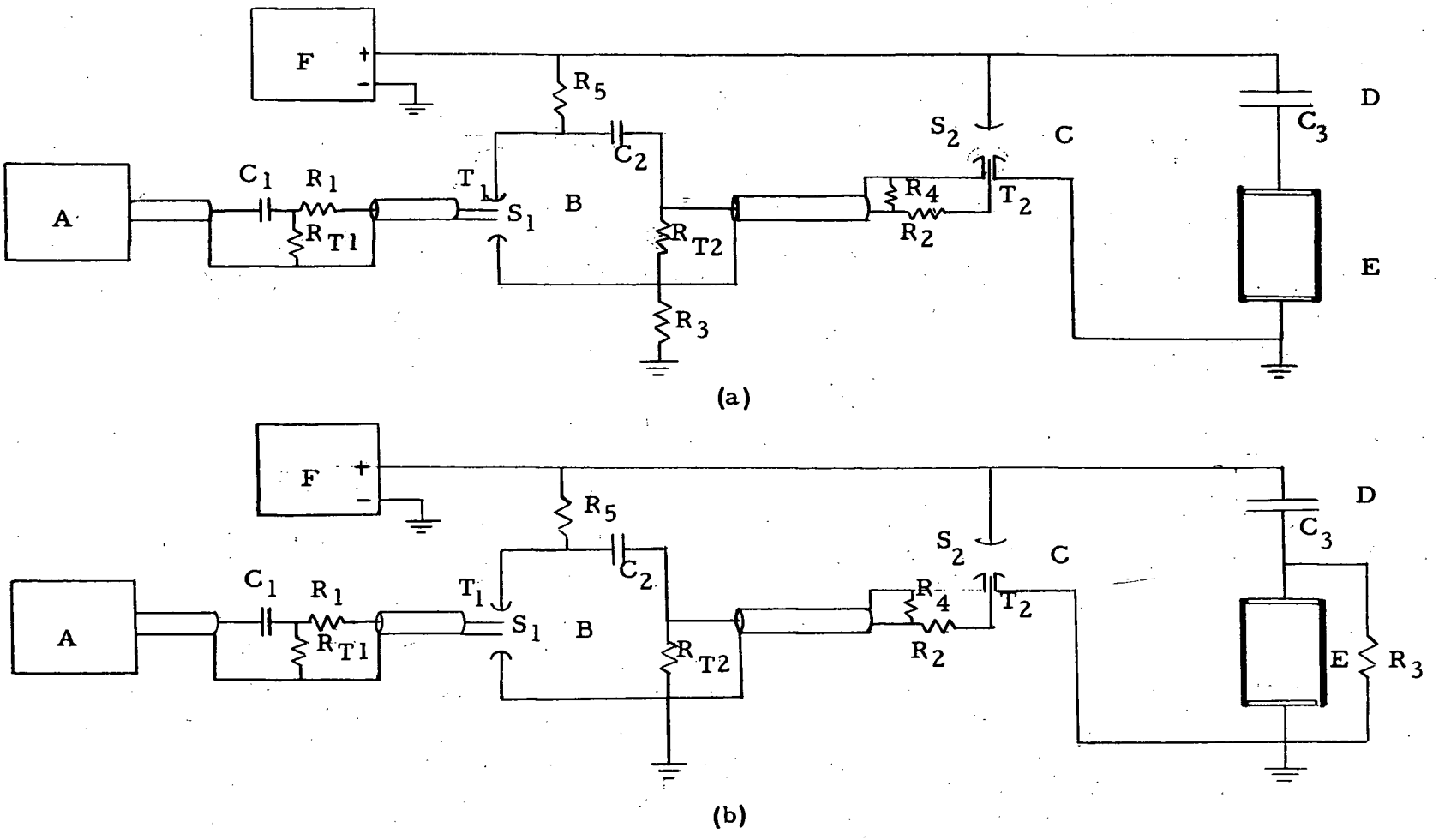

Figure 3: Circuit Diagrams

A, Thyratron trigger unit; B, Trigger generator; C, Three electrode spark gap switch; D, Capacitor bank; E, Discharge vessel; F, 12 kV power supply; R_1, R_2 (680 Ω), Damping resistors; R_{T1} (170 kΩ), R_{T2} (50 Ω), Terminating resistors; R_3 (100 kΩ); R_4 (50 Ω); R_5 (200 kΩ); T_1, T_2 Trigger spark gaps; S_1, S_2 Current switches; C_1 (500 pF), C_2 (.06 μF); C_3 (15 μF); a, Original circuit; b, Final circuit.

The grounding connections indicated in figure 3 are made to brass plates buried under the laboratory floor.

Originally, the trigger generator (B) was grounded as shown in figure 3a, page 6. This connection provided a completely coaxial system and thus provided a minimum of radiated noise signals. However, the trigger generator did not trigger reliably when connected in this way and it was necessary to use the circuit of figure 3b. This circuit does not provide a shield for the 700 ohm resistor (R_2) in the trigger lead. Therefore, the noise radiated from this lead is greater for circuit (b) of figure 3 than for circuit (a). The circuit in figure 3b triggers more readily because in this case the potential difference across the gap (S_2) is increased by the trigger pulse, whereas in figure 3b, the potential difference is reduced. The larger the potential difference across the gap, the easier it breaks down.

The components of the discharge circuit will now be discussed individually and in considerable detail so that the equipment could be reproduced if desired.

2.1 THYRATRON TRIGGER UNIT AND THEOPHANIS TERMINATOR

The complete circuit of the thyratron trigger unit is shown in figure 4, page 8, although an external 300 volt power supply is also required. Upon triggering, a 9.5 kV negative pulse is transmitted down the charged output cable. The output cable is a 6 foot length of RG 58/U coaxial cable. It is terminated by a unit developed from a design by Theophanis (1960) which presents a large impedance to the negative pulse and thus doubles the amplitude of the pulse upon

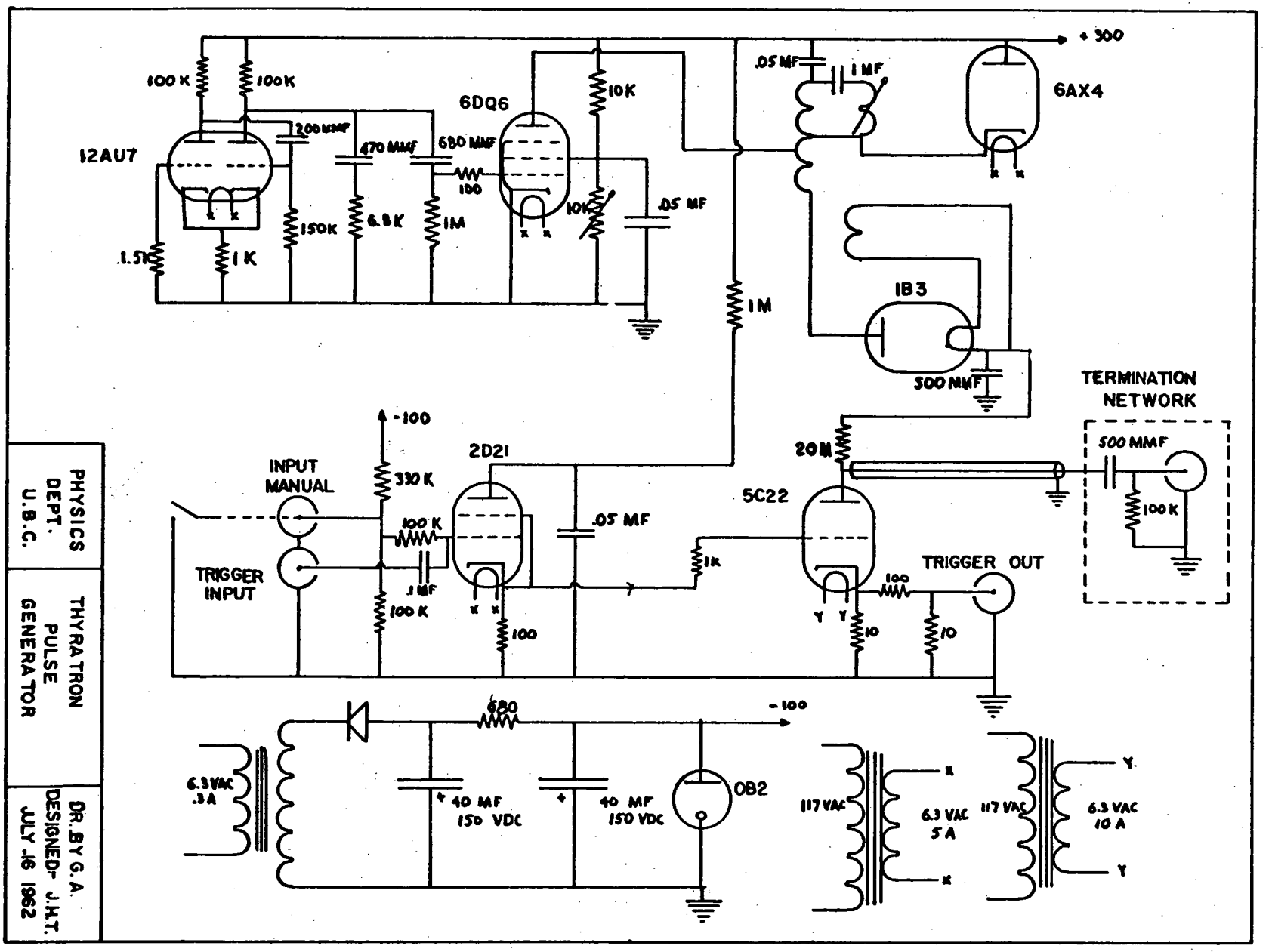
+300
100K
100K
12AU7
200 MMF
470 MMF
680 MMF
100
150K
6.8K
1M
1.5K
1K
6DQ6
10K
10K
.05 MF
.05 MF
1 MF
6AX4
1M
1B3
500 MMF
TERMINATION NETWORK
-100
INPUT MANUAL
330K
2D21
20M
5C22
500 MMF
100K
.05 MF
TRIGGER INPUT
100K
.1 MF
100K
100
1K
100
TRIGGER OUT
10
10
680
-100
6.3 VAC .3A
40 MF 150 VDC
40 MF 150 VDC
0B2
117 VAC
6.3 VAC 5 A
117 VAC
6.3 VAC 10 A
PHYSICS DEPT. U.B.C.
THYRATRON PULSE GENERATOR
DR. BY G.A. DESIGNED J.H.T. JULY 16 1962

reflection. The output of the terminator is a 19 kV negative pulse with a 40 nsec rise time. By experiment, the optimum value of the termination resistance (R_{T_1} of figure 3, page 6) has been found to be 140-170 kilo-ohms. This is determined by mounting a search coil around the spark gap (T_1 of figure 3) and observing the resulting signal on an oscilloscope. Resistances larger than 170 kilo-ohms produce appreciable oscillations in the circuit for up to 1 microsecond following the pulse while resistances smaller than 140 kilo-ohms give insufficient spark for reliable triggering of the spark gap switch (S_1 of figure 3).

The possibility of emission of radio frequency noise signals by both the trigger unit and the terminator has been reduced to a minimum by careful construction, including complete screening of the 5C22 thyratron tube.

2.2 TRIGGER GENERATOR

As described in section 2.0, page 4, the important feature of the trigger generator is the achievement of complete isolation between the triggering electronics and the high voltage discharge circuit. The generator is of coaxial construction as shown in figure 5, page 10, and the operation of the generator is as follows (see also figure 3, page 6). The thyratron trigger unit of subsection 2.1, page 7, provides the energy for the trigger spark (T_1) which triggers the switch (S_1). The trigger spark (T_1) is enclosed in a quartz bulb and is thus completely isolated, electronically, from the switch (S_1). However, the ultraviolet light radiated from the spark (T_1) produces enough photo-electrons in the gap (S_1) to result in breakdown. This system provides complete d.c.

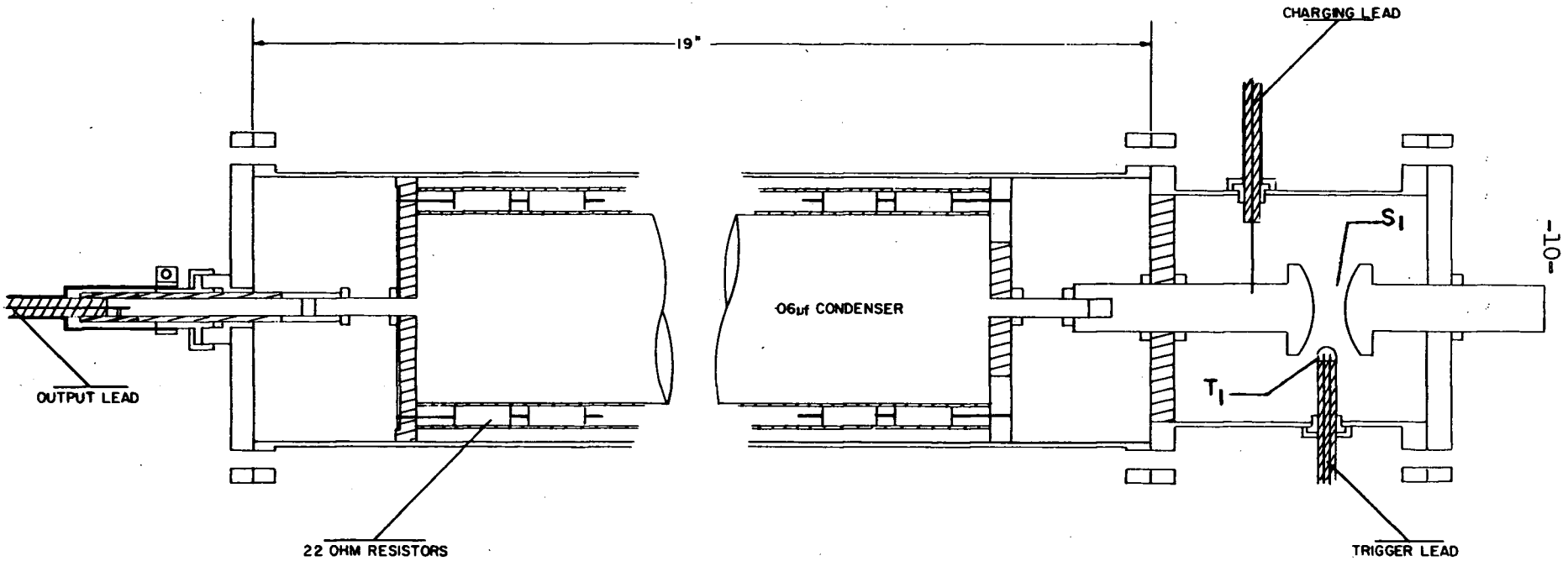

FIGURE 5

TRIGGER GENERATOR

SCALE : HALF SIZE

SHADED PORTIONS REPRESENT PLASTICS,
REMAINDER CONSTRUCTED OF BRASS

isolation between the trigger unit (A) and the discharge circuit (C, D, E) (see figure 3, page 6). It also provides excellent a.c. isolation because of the low capacity between the spark gaps (T_1) and (S_1).

As pointed out by Curzon and Smy (1961), the potential across the spark gap (S_1) has to be within 4% of the breakdown voltage of the gap for this triggering method to work. For this reason, the main capacitor bank (C_3) and the trigger generator capacitor (C_2) are connected in parallel. In this way, the large capacitance of the main bank stabilizes the potential across the spark gap (S_1). Otherwise, leakage from the relatively small trigger generator capacitor would make it difficult to stay within the 4% voltage margin necessary for successful triggering of the trigger generator.

As a secondary result, the parallel connection mentioned above ensures a constant firing voltage of the main bank (within 4%). This occurs because the main capacitor bank (C_3) and the trigger generator capacitor are charged in parallel from the same power supply (F), as shown in figure 3, page 6. The firing voltage of the main bank is determined, therefore, by the setting of the trigger generator spark gap (S_1). In the present investigation, all work is done with the capacitor bank charged to 12 kV and the spark gap separation (S_1) is set only once for the entire experiment.

The output pulse from the trigger generator is taken across the resistance (R_{T2}) which has a value of 50 Ω in order to match the output cable properly.

The trigger generator is robust, has low jitter times which are

the order of nanoseconds, and the delay between the triggering of the thyratron and the firing of the trigger spark (T_2) in the main spark gap (S_2) is of the order of 10 nsec. (Curzon and Smy (1961)).

Another advantage of the trigger generator and discharge circuit is that it operates in optimum conditions whether a positive or negative charging potential is used. It is known that the best triggering conditions are achieved when the trigger pulse is of opposite polarity to the high voltage electrode (see page 179 of Meek and Craggs (1954)). The trigger generator described here provides this relationship for the cases of either positive or negative charging potentials. All that is necessary is to set the polarity of the power supply. A trigger pulse of the correct polarity for optimum triggering conditions is then automatically produced by the triggering circuit.

The capacitance and inductance of the trigger generator are determined by shock exciting the circuit. This method consists of observing the ringing frequency of a circuit which is excited by suddenly applying an e.m.f. to its output terminals.

In the present case, the spark gap switch (S_1) was shorted out and a small battery was connected across the output terminals of the trigger generator (i.e. across R_{T2} of figure 3b, page 6). A small seach coil was wound around one of the output leads to pick up the resulting signal.

Using the above arrangement, the period (T) of the signal produced by ringing of the circuit due to its natural reactance was measured. Also the period (T') of the ringing which results when the natural capacitance (C) of the circuit is augmented by a known capacitance (C_o) was measured. Then the inductance (L) and capacitance (C) of the

circuit were calculated using the following equations:

$$LC = \left[\frac{T}{2\pi}\right]^2$$

$$L(C+C_o) = \left[\frac{T'}{2\pi}\right]^2$$

where L = inductance of the trigger generator

C = capacitance of the trigger generator

C_o = known capacitance placed in parallel with the circuit and battery

T = period of the signal without the additional capacitance C_o

T' = period of the signal with the additional capacitance C_o

For the trigger generator described above, the capacitance was 0.06 pF and the inductance was 5 nH.

2.3 CAPACITOR BANK AND DISCHARGE SWITCH

Two G.E. "Pyranol" storage capacitors rated at 20 kV D.C. are used as the capacitor bank. The capacitors are connected in parallel and they have a capacitance of 7.5 pF each.

The discharge switch, or the main spark gap switch (S_2 of figure 3, page 6), is mounted above the capacitors as shown in figure 6a on page 14. Electrically, the switch is connected in series between the capacitor

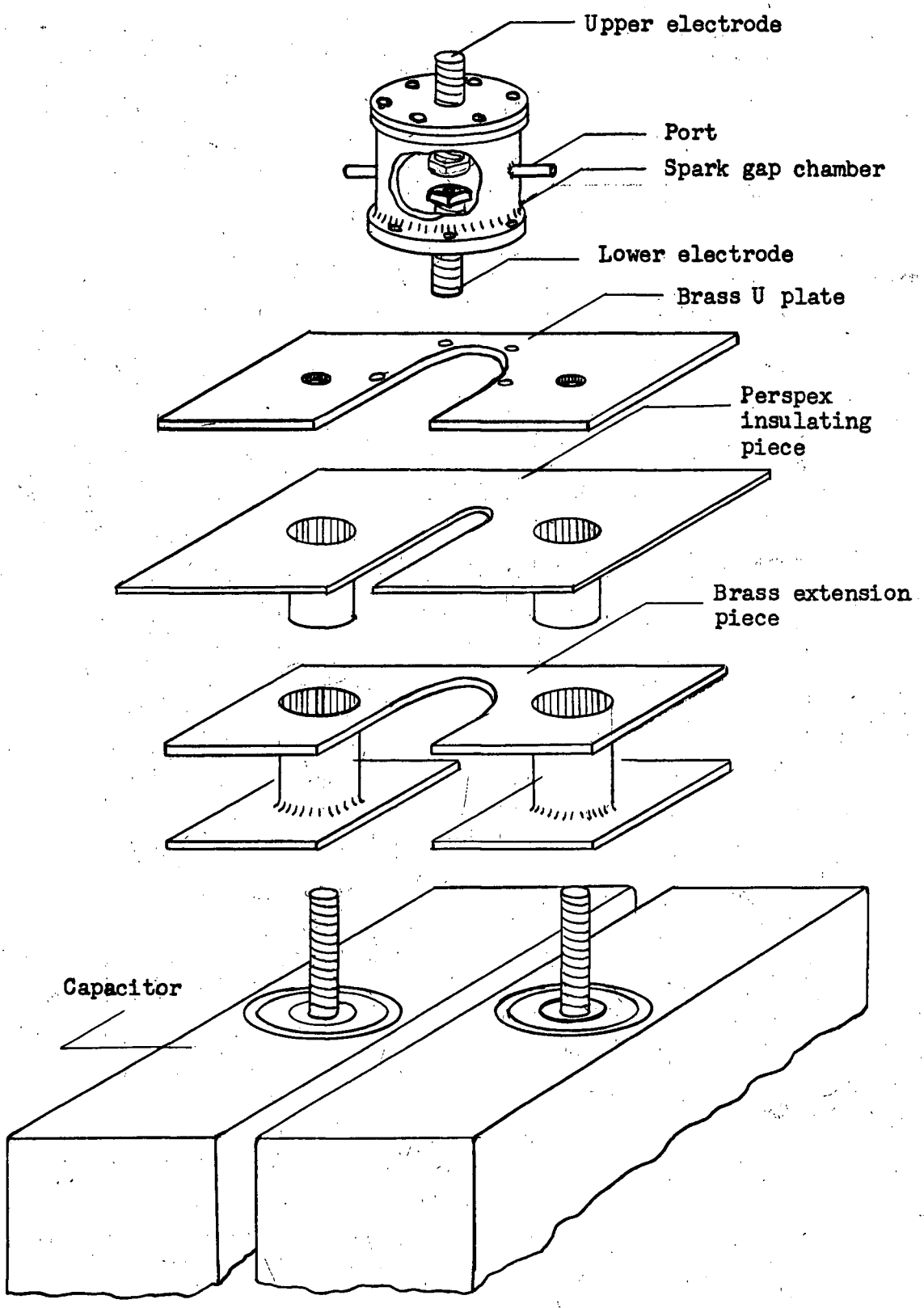

Figure 6a: Main Spark Gap Switch Assembly

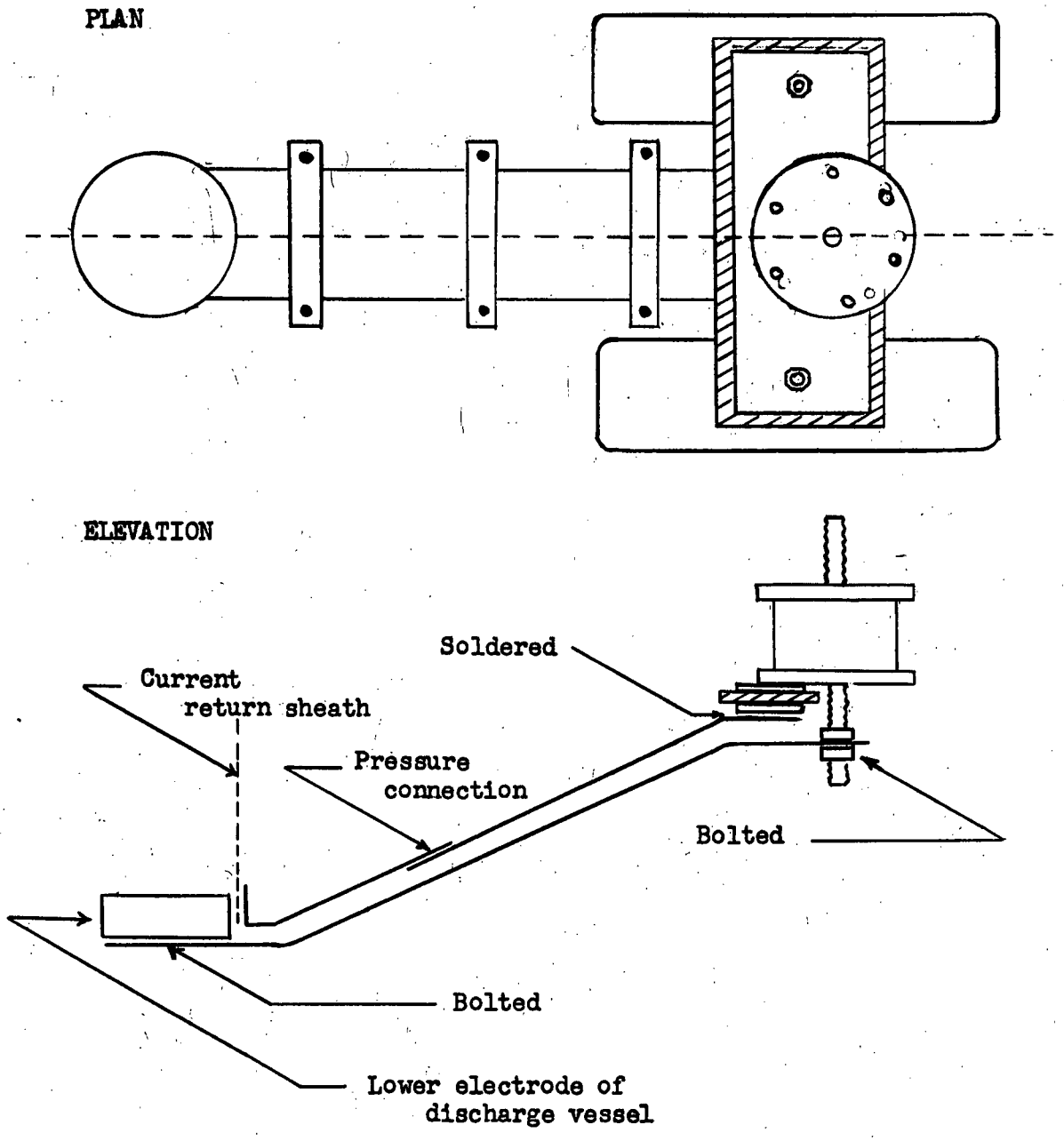

Figure 6b: Lead Connections (from main capacitor bank to discharge vessel)

bank and the discharge vessel.

Two ports have been built into the walls of the spark gap chamber to accommodate equipment for pressurizing the spark gap chamber.

The high voltage electrode of the discharge switch (upper electrode of figure 6a) can be at either positive or negative potential depending upon the polarity of the high voltage power supply. The low voltage electrode of the discharge switch contains the trigger pin which is energized by the trigger generator of page 9.

Details of the electrodes used on the discharge switch are shown in figure 7, page 16. The electrode heads can be unscrewed from the electrode shafts to facilitate interchanging various types of electrodes, if required. An axial hole in the upper electrode seems to improve the triggering reliability of the switch. The trigger pin is made from 0.02 inch tungsten wire and it is insulated with polyethylene tubing and fitted into an axial hole in the low voltage electrode. A paxolin cylinder is placed over the polyethylene insulation at the trigger pin tip in order to reduce damage to the insulation caused by the trigger spark. The height of the trigger pin relative to the surface of the electrode can be adjusted.

Two flat copper leads 10 cm. in width, 80 cm. in length and separated by 3 mm of polyethylene carry the current from the capacitor bank and discharge switch to the discharge vessel. These leads are connected as shown in figure 6b, page 14(a).

This is an opportune place to point out that whenever metal parts are joined by a pressure connection, the contacting surfaces are heavily tinned with soft solder. The solder seals gaps where arcing occurs and

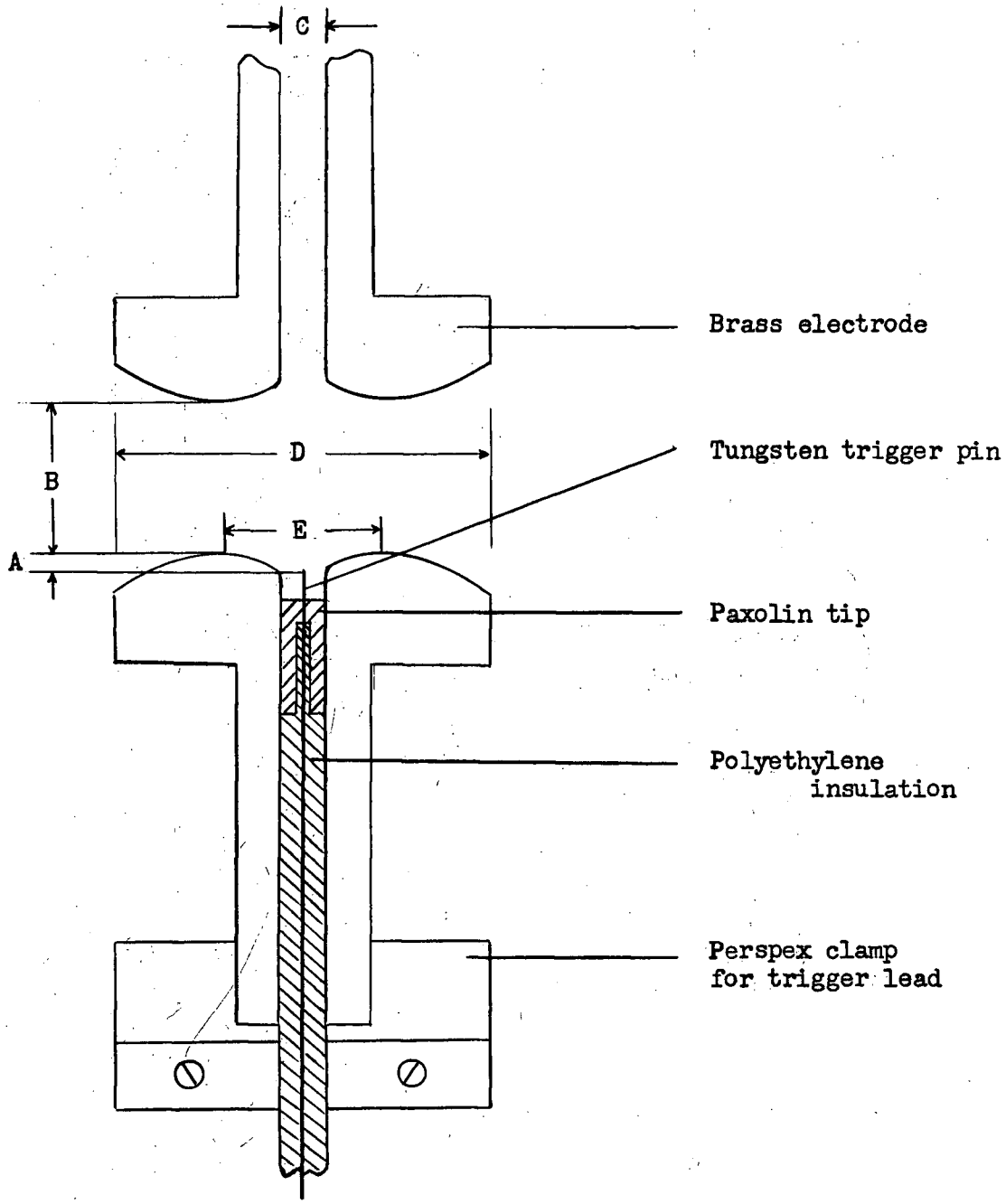

Figure 7: Spark Gap Electrodes

A, Distance of trigger pin below electrode face (1 mm); B, Gap separation (11 mm); C, Diameter of axial hole (4 mm); D, Diameter of electrode (25 mm); E, Diameter of highest portion of electrode face (10 mm).

leaves a noise free pressure connection.

It is also noted that when the discharge circuit is not being operated, the terminals of the capacitor bank shown on page 14 are shorted to ground through a safety switch.

By shock exciting the bank and leads in the manner described on page 12, the capacitance of the bank is found to be 15 pF and the inductance, including leads, is found to be 0.11 μH. By calculation, the capacitance of the leads is found to be 300 pF.

2.4 DISCHARGE VESSEL

A diagram of the discharge vessel is given in figure 8, page 18. The electrodes, which are made of brass, are 7.6 cm in diameter at the electrode face and are separated by a distance of 33 cm. The upper electrode is designed to permit end on observation of the discharge while the current return sheath is made of brass mesh to permit side on observation of the discharge.

From the dimensions of the discharge vessel, its capacitance and inductance are calculated to be 1.2 pF and 40 nH respectively.

The upper electrode is constructed such that a Rogowski coil can be placed around it in order to measure the discharge current.

The discharge vessel is evacuated through an outlet in the lower electrode. The vacuum system is fitted with a "Vacustat" for pressure measurement, and it is also provided with facilities which enable the discharge vessel to be filled with individual gases or mixtures of gases. In practice, for the experiment reported here, the discharge vessel was filled with air at pressures between 0.6 and 1 mm Hg.

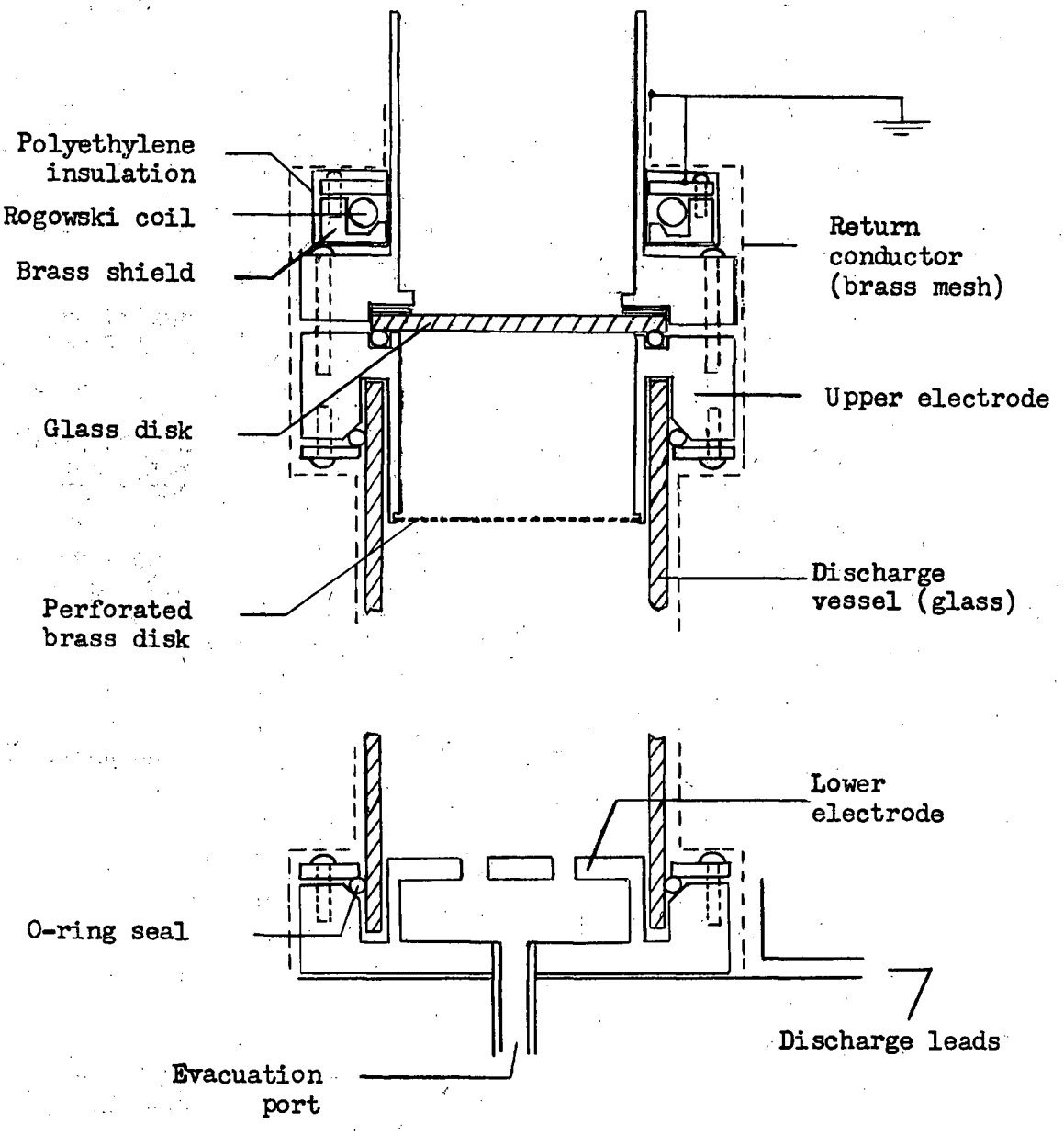

Figure 8: Discharge Vessel

3.0 MEASURING DEVICES

The discharge current can be measured in a number of ways, the most common methods being with magnetic probes (Lovberg (1959)), Rogowski coils (Golovin et. al. (1958)) and the current shunt (Meek and Craggs (1954)).

In the present investigation, as the reduction of noise signals is of utmost importance, the Rogowski coil is chosen as the method of obtaining current measurement. The Rogowski coil has a favourable signal to noise ratio and it is easily constructed.

A detailed description of the Rogowski coil and its associated circuitry is given in this section. The basic feature underlying the design of the measuring circuit is complete impedance balance. The expression "complete impedance balance" means that the impedance of the measuring circuit as seen out of either terminal of the Rogowski coil is the same. Signals picked up by the measuring circuit are then attenuated equally down each leg of the measuring circuit.

At this point it is convenient to introduce certain terms which are used subsequently in the description of the measuring devices and also in the discussion of the investigation of noise signals presented in subsection 4.0, page 37.

The means by which noise signals enter the measuring circuit can be characterized as either inductive or capacitative pick up.

The term "inductive pick up" is associated with coupling between the measuring and discharge circuits due to conduction currents. For example, referring to figure 9, page 20, a time varying conduction current flowing in circuit 2 induces an e.m.f. in circuit 1 through the

mutual inductance between the two circuits.

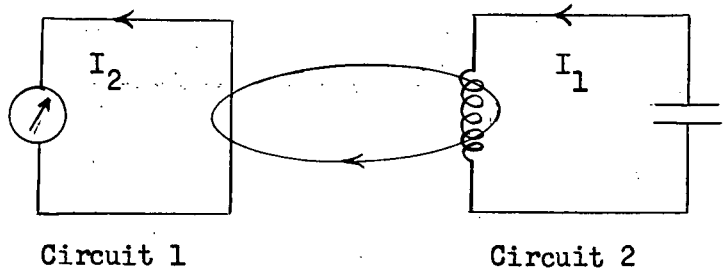

Figure 9: Illustration of Inductive Coupling

A "ground loop" is a complete electrical path joining any two earthed points in a circuit. In practice, conduction currents in undesirable ground loops are sources of spurious noise signals, because of the self inductance of such loops.

The term "capacitative pick up" refers to coupling between the measuring and discharge circuits which is associated with displacement currents. Charge fluctuations on spark gap electrodes, for example, produce time varying electric fields which may be picked up on the surface of any metal object in the vicinity of the spark gap.

The term "radiative pick up" embraces pick up of both the inductive and capacitative types.

3.1 ROGOWSKI COIL

A Rogowski coil is a form of current transformer where the secondary is a toroidally wound coil through which the main discharge current - the primary - is threaded. The coil is made from a single loop of

RG 65 A/U delay line with the outer screening removed. It is mounted in a slotted brass can (see figure 8, page 18) which is isolated from the coil and then grounded to reduce capacitative coupling between the discharge electrodes and the coil. For convenience, the coil is placed around the upper electrode of the discharge vessel and to minimize capacitative pick up the ground for the discharge circuit is connected to the top of the tube, very close to the coil. By using this grounding procedure, the potential difference between the current return sheath outside the coil and the electrode inside the coil is kept very small. The potential difference between the current return sheath and the lower electrode can range in values up to 5.0 kV due to the inductance of the discharge vessel.

The induced voltage in the Rogowski coil (V_c) can be determined from the following expression:

$$V_c = - \frac{a N \mu}{4\pi R} \frac{dI}{dt}$$

$$= - 2.1 \times 10^{-8} \frac{dI}{dt} \text{ volts}$$

where a = area of coil winding = $\pi (1.6 \times 10^{-3})^2$ m^2

R = radius of torus = 4.9×10^{-2} m

N = number of turns = 1300

I = discharge current in amps.

Peak currents of the order of 10^5 amps. are obtained in times of the order of 10^{-6} seconds and these currents, therefore, produce peak voltages of the order of 10^3 volts at the output terminals of the Rogowski coil.

3.2 MAXIMALLY FLAT FREQUENCY RESPONSE

In general, the voltage (V_c) induced in the Rogowski coil is not measured directly. Instead, one measures V_o, some potential generated in an external circuit by the induced e.m.f. (V_c). It is convenient to use a system where V_o is directly proportional to V_c, independent of frequency. A system for which this condition obtains over as broad a frequency range as possible is said to be maximally flat.

It can be shown (Segre (1960)) that

$$V_o = k V_c$$

where k is a constant when the external impedance presented to the output terminals of the Rogowski coil is equal to the characteristic impedance of the coil. The characteristic impedance (R_c) of the coil is given by

$$R_c = \sqrt{\frac{L}{2C_c}}$$

where L = inductance of the coil

C_c = capacitance of the coil.

If the coil feeds an impedance considerably smaller than its own characteristic impedance, the higher frequencies are attenuated; however, if the coil feeds an impedance considerably greater than its characteristic impedance, there is a pronounced increase in gain at the resonant frequency (ω_R) of the coil $\left(\omega_R = \frac{1}{\sqrt{LC_c}}\right)$.

In order to determine the characteristic impedance of the coil, the circuit of figure 10a, page 24, was shock excited in the manner described on page 12. The period (T) of the ringing signal was observed on an oscilloscope and found to be 0.17 μsec. Similarly, with a 47 pF capacitance across the output terminals of the coil, a period (T') of 0.35 μsec. was observed. Thus

$$LC_c = \left[\frac{T}{2\pi}\right]^2 = 7.32 \times 10^{-16} \text{ sec}^2$$

$$L(C_c + 47 \text{ pF}) = \left[\frac{T'}{2\pi}\right]^2 = 31.0 \times 10^{-16} \text{ sec}^2$$

from which it follows that

$$L = 50 \mu H$$

$$C_c = 15 \text{ pF} .$$

The characteristic impedance is then given by

$$R_c = \sqrt{\frac{L}{2C_c}} = 1300 \text{ ohms} .$$

A resistance (R_T) of 100 ohms is required in terminating the signal cable. The remainder of the required matching impedance (1300 ohms) is made up of two 600 ohm resistances (R_m), one in each leg of the measuring circuit to preserve impedance balance.

The matching resistances (R_m) and the terminating resistance (R_T) are placed at the coil end of the signal cable and they are contained in a small brass can to minimize capacitative and inductive coupling between

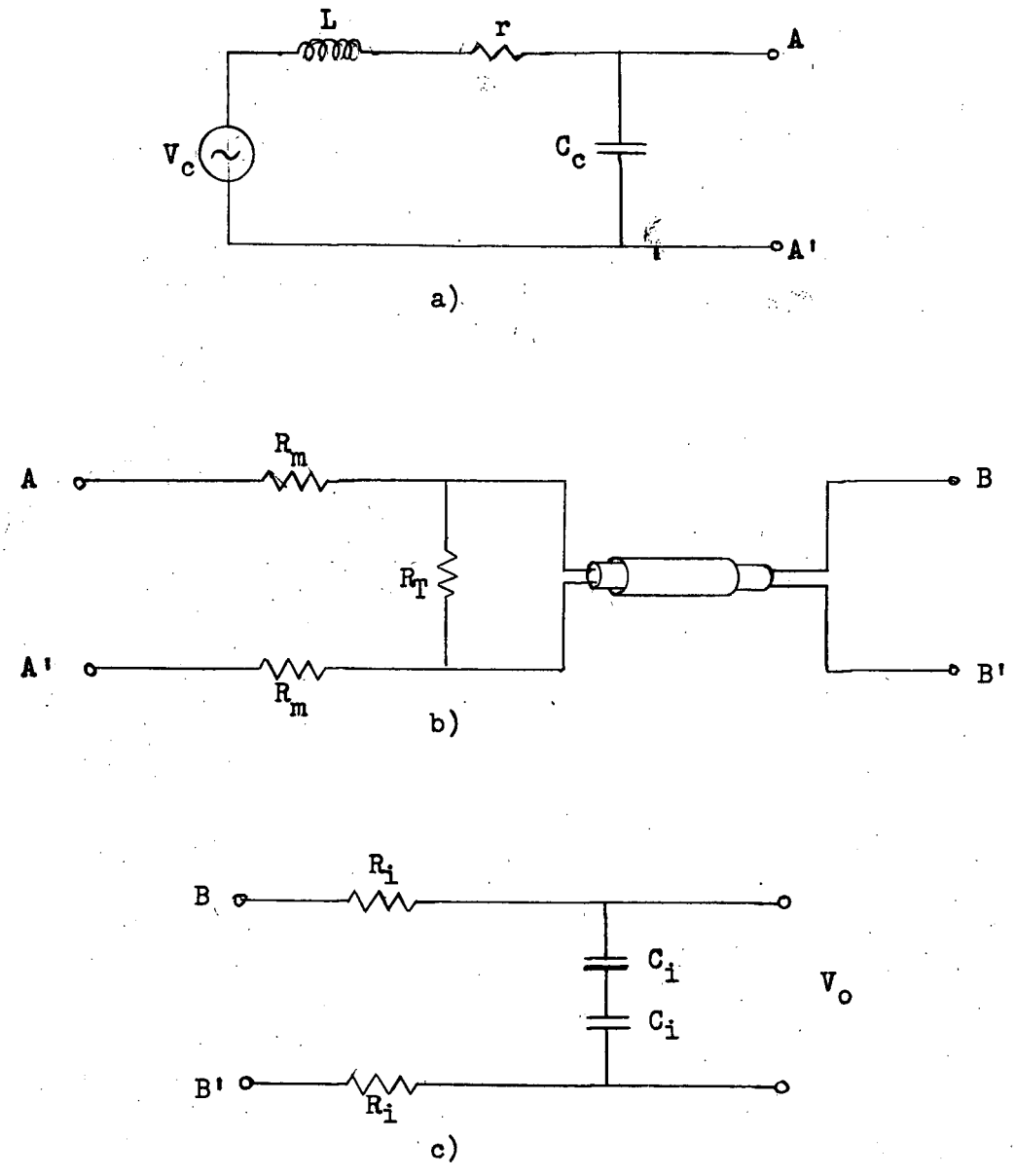

Figure 10: Rogowski Coil Measuring Circuit

a) Rogowski coil equivalent circuit; L (50 μH), coil inductance; r(10 Ω), coil resistance; C_c (15 pF), coil capacitance; V_c, induced coil voltage.

b) Matching network and signal cable: R_T (100 Ω) cable terminating resistance; R_m (600 Ω), coil matching resistances; signal cable, RG 22/U.

c) Integrating network ; R_i (18 kΩ), C_i (0.01 pF); V_o, output voltage.

the measuring and discharge circuits.

Segre (1960) gives the ratio (A) of, and the phase difference (ϕ) between, the output and input voltages associated with a circuit such as shown in figure 10a,b on page 24 as

$$|A|^{-2} = \left[\frac{R+r}{R}\right]^2 + \Omega^4 - \Omega^2\left[2 - \frac{r^2}{R_o^2} - \frac{R_o^2}{R^2}\right]$$

$$\phi = \tan^{-1}\left[\frac{\Omega}{\Omega^2 - \frac{r+R}{R}}\left(\frac{R_o}{R} + \frac{r}{R_o}\right)\right]$$

where $\Omega = \omega\sqrt{LC_c}$

$R = R_T + 2\,R_m$

$R_o = \sqrt{\frac{L}{C_c}}$

and the remaining symbols pertain to figure 10a,b.

Substituting the actual values for the Rogowski coil measuring circuit into these relations it is found that the 3 db point of the response curve occurs at $f = 6$ Mc/s. This is to be compared with the discharge frequency of 0.1 Mc/s.

From the above formula, the phase angle ϕ for the discharge frequency of 0.1 Mc/s amounts to -8' which is negligibly small.

3.3 INTEGRATOR

The output voltage (V_c) of the Rogowski coil is given by

$$V_c = -2.1 \times 10^{-8}\,\frac{dI}{dt}\ \text{volts}$$

(see page 21). When this voltage is integrated, a signal is obtained which is proportional to the discharge current.

The integrator used is a simple RC circuit (shown in figure 11) for which the integration condition is $RC >> T$, where T is the period of the signal to be integrated. In the present discharge circuit the

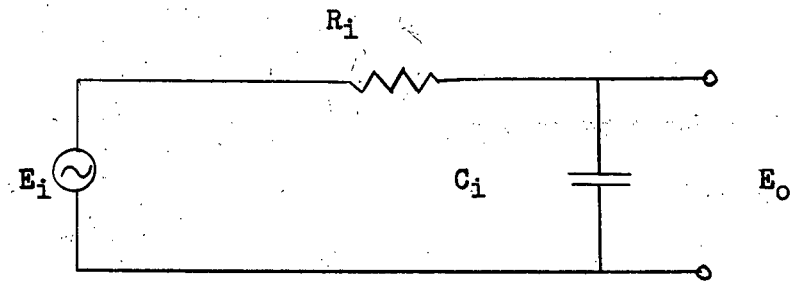

Figure 11: Integrating Circuit

current lasts for approximately 3 cycles and oscillates with a period of approximately 10 μsec. An integration constant (RC) of 180 μsec. was chosen, i.e. $R_i = 18\ k\Omega$ and $C_i = 0.01$ pF.

In the circuit of figure 10c, page 24, two such integrators are used so as to preserve the balanced design of the measuring circuit. The integrators are mounted in brass cans (shown in figure 31, page 62) which serve to minimize radiative coupling between the measuring and discharge circuits. (For an important note concerning the construction of the integrators, see page 63.)

The complete measuring circuit is formed by combining the circuits of figure 9, page 20. The action of the complete measuring circuit may be summarized by considering its transfer function which, written in the usual Laplace transform notation (i.e. $s = j\omega$) is:

$$\frac{V_o}{V_c} = \left[\frac{1}{\frac{R+r}{R} + \left(\frac{L}{R} + C_c r\right) s + C_c L s^2}\right] \cdot \left[\frac{R_T}{R_T + 2Rm}\right] \cdot \left[\frac{1}{sR_i C_i + 1}\right]$$

where $R = R_T + 2Rm$

and the remaining symbols refer to figure 10, page 24. It should be noted that this equality is valid only if the shunt impedance of the signal cable is small compared with the impedance of the integrators; that is, $R_T << 2\left[R_i + \frac{1}{sC_i}\right]$.

More simply,

$$\frac{V_o}{V_c} \sim \frac{R_T}{R_T + 2Rm} \cdot \frac{1}{R_i C_i} \cdot \frac{1}{s}$$

where the approximation is valid if

$$R_T + 2R_m > r$$

$$\frac{L}{R} + C_c r < T$$

$$C_c L < T^2$$

$$R_i C_i > T$$

and where T is the period of the observed signal. Inverting this transform shows that the output voltage from the measuring circuit is

directly proportional to the integral of the voltage (V_c) induced in the Rogowski coil. However, the induced voltage (V_c) is directly proportional to the time derivative of the discharge current (see page 21). Therefore, the output voltage from the Rogowski coil measuring circuit is directly proportional to the discharge current.

3.4 FREQUENCY RESPONSE OF MEASURING CIRCUIT

The measurement of the discharge current obtained using the Rogowski coil measuring circuit of figure 10, page 24, is accompanied by a noise signal which is characterized by certain well defined frequencies. As mentioned previously, the noise investigation presented in this thesis is concerned, in part, with discovering if this noise signal is due to fluctuations in the discharge current. To discover this, it is first necessary to establish that the bandwidth of the Rogowski coil measuring circuit is sufficient to pass those frequencies which characterize the noise signal. For this reason, the frequency response of the Rogowski coil measuring circuit is determined experimentally. The frequency response of two other circuits used in the noise investigation is measured as well. The two circuits in question are simple modifications of the Rogowski coil measuring circuit made in one case by removing the integrating network from the circuit and in the other case by adding a delay line to the circuit. The procedure used in measuring the frequency response of these circuits is discussed in this subsection in considerable detail.

The circuitry involved in the frequency response measurements is shown in figure 12, page 29. For convenience, the circuitry has been separated into four parts.

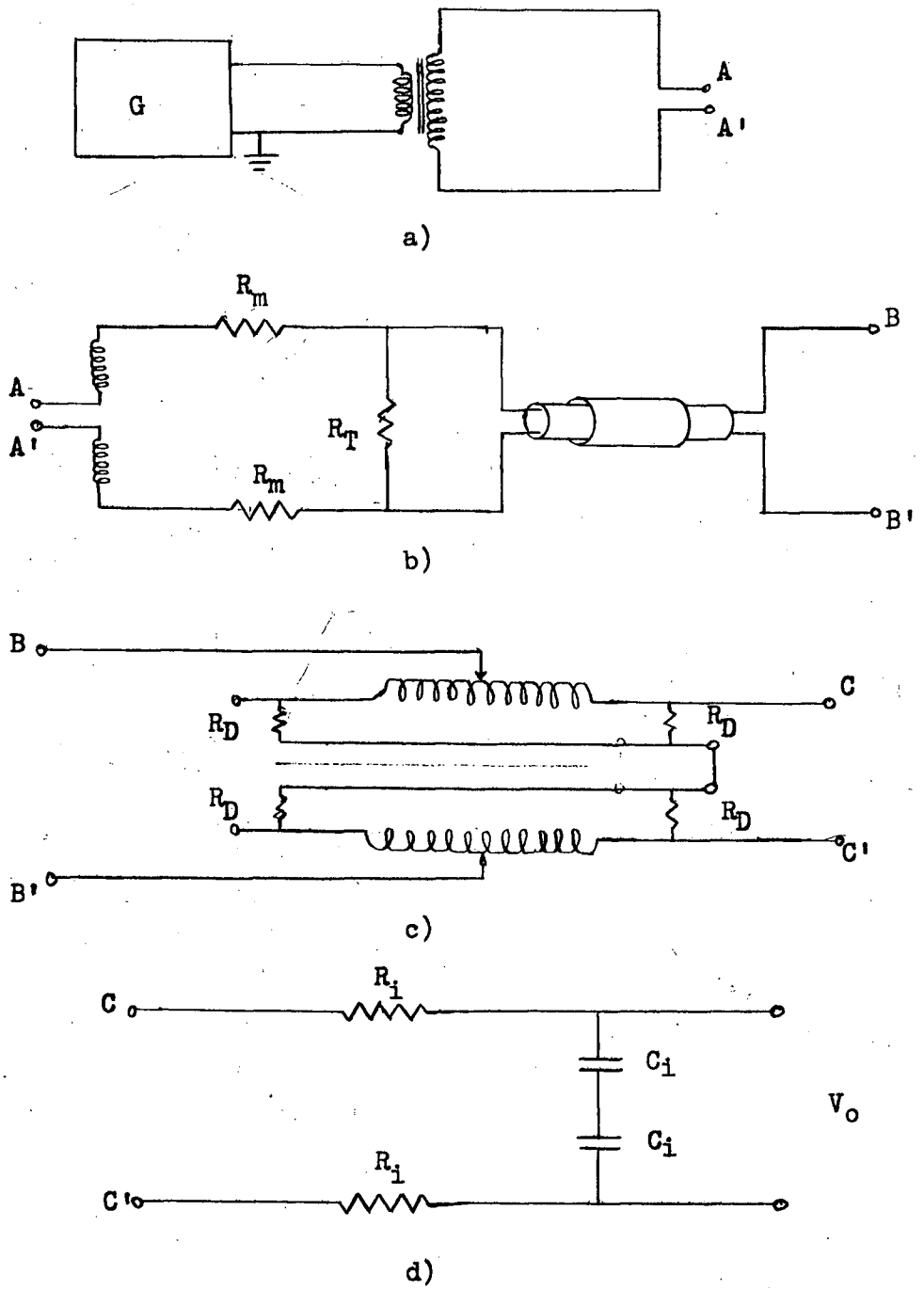

Figure 12: Circuitry for Measuring Frequency Response

a) Floating signal source; G, Tektronix Type 190B constant amplitude sine-wave generator; b) Rogowski coil and signal cable; R_m (variously 600, 800 or 1000 Ω) matching impedance; R_T (100 Ω) terminating impedance; c) General Radio Type 314-S86 delay lines; R_D (220 Ω) matching resistors; d) Integrating network; R_i (18 kΩ), C_i (.01 pF).

The signal source (G) in a) of figure 12 is a Tektronix Type 190B constant amplitude sine-wave generator. According to specifications published by Tektronix, this signal generator will deliver a 10 volt peak-to-peak signal which varies in amplitude by less than ±2% from 50 Kc/s through 30 Mc/s, provided the load shunt capacitance does not exceed 10 pF. The output from this generator is unbalanced; that is, one side of the output terminal is grounded. In practice, however, the measuring circuit is floating; that is, no point in the circuit is held at some fixed potential. In order to duplicate, as closely as possible, the actual operating conditions of the measuring circuit while determining its frequency response, a floating signal source was constructed. The floating signal source is shown in a) of figure 12 and consists of the above mentioned signal generator feeding a matching transformer. The matching transformer consists of a small, high quality ferrite torus wound with #26 AWG enamelled copper wire in a turns ratio of 1:2. The ferrite torus and windings are enclosed in a small brass can to minimize the magnetic field radiated from the transformer.

The output signal from the matching transformer (AA') is fed into the measuring circuit by cutting the RG 65 A/U cable forming the Rogowski coil into two equal parts and making the connections as indicated in b) of figure 12. All the remaining components in figure 12, except for c), have been discussed in subsection 3.2 (see page 24).

Circuit c) represents two General Radio Type 314-S86 variable delay lines which provide a maximum delay of 0.5 μsec. each. The delay lines are connected in parallel, as shown, in order to preserve the balanced design of the measuring circuit. Four 220 ohm resistors, two in each

delay line, provide the proper matching impedance for the delay lines.

The signal from the matching transformer (AA') and the signal from the particular circuit whose frequency response is being measured are displayed simultaneously using a Tektronix Type 551 dual beam oscilloscope. In this way, loading conditions on the signal source remain unchanged throughout the measuring operation. The signal from the matching transformer (AA') is fed, via two Type P6006 Tektronix probes, to a Tektronix Type G balanced differential preamplifier. The signal from the circuit whose frequency response is being measured is fed directly to a second Tektronix Type G balanced differential preamplifier. (The latter differential preamplifier is the same one used throughout the noise investigation).

The procedure used in measuring the frequency response will be described now for a particular arrangement consisting of the floating signal source (a) feeding the Rogowski coil and signal cable (b) of figure 12. The attenuation settings of the preamplifiers which received the signals from (AA'), (BB') were adjusted to 0.5 v/cm and 0.2 v/cm, respectively. Both attenuation settings remained unchanged throughout the measuring operation. The sweep speed was fixed at 5 msec/cm for the entire measuring operation in order to avoid errors in measuring the trace amplitudes due to 60 cps hum. (The 60 cps signal was less than 5 mv or, typically, about 1% of the amplitude of the measured signal). The frequency of the signal from the generator was set to 0.05 Mc/s and the output amplitude was adjusted to produce a 10 volt signal at (AA'), as measured from the oscilloscope display. Then the amplitude of the signal at (BB') was measured. This procedure was repeated for various

frequency settings of the generator from 0.05 Mc/s to 50 Mc/s.

The same procedure was repeated for two other arrangements which consisted of the Rogowski coil and cable and delay lines in one case and of the integrator alone in the other case.

The frequency response could not be measured for the total system consisting of the Rogowski coil, signal cable, delay lines and integrator because, with the signal source available, the output from this system was too small to make reliable measurements. However, the frequency response of the total system mentioned above can be obtained by a) measuring the frequency response of the total system but with the integrator removed, b) measuring the frequency response of the integrator alone and c) taking the product of these two response measurements. It must be noted that this procedure is valid only because the shunt impedance of the integrator is large compared with the shunt impedance of the preceding circuitry.

Finally, a check was made to determine if the ratio of the attenuations of the two preamplifiers was independent of frequency. This was done by fixing the output from the signal generator at a convenient value and then measuring the amplitude of the signal at (AA') for frequency settings from 0.05 Mc/s through 30 Mc/s, using first the preamplifier with the 0.2 v/cm attenuator setting and then the preamplifier with the 0.5 v/cm attenuation setting. The ratio $\frac{0.2\ \text{v/cm}}{0.5\ \text{v/cm}}$ was up by 5% at 15 Mc/s and by 15% at 30 Mc/s from the value at 0.05 Mc/s (0.41). No corrections were made on the frequency response measurements discussed above since frequencies above 15 Mc/s are of little interest as far as the response of the measuring circuits is

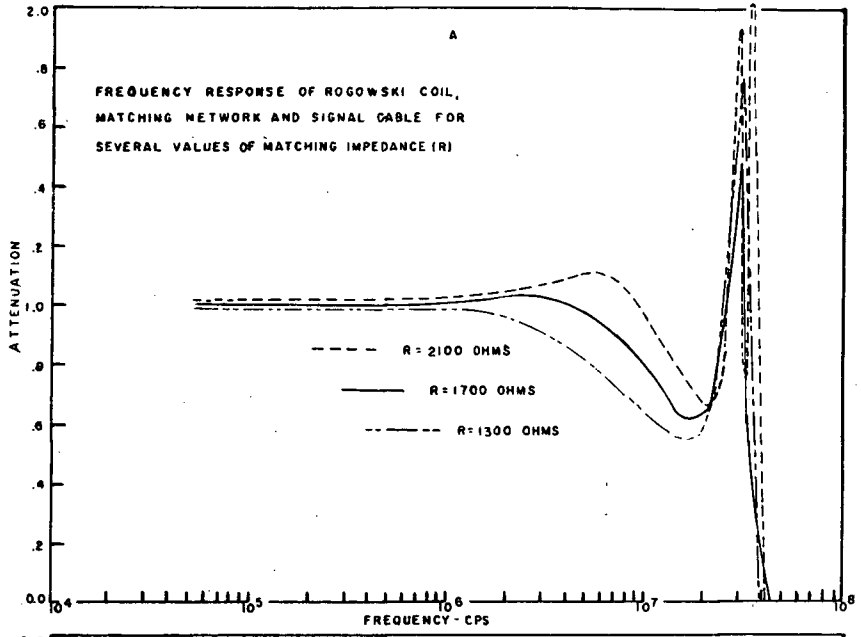
A
FREQUENCY RESPONSE OF ROGOWSKI COIL, MATCHING NETWORK AND SIGNAL CABLE FOR SEVERAL VALUES OF MATCHING IMPEDANCE (R)
R = 2100 OHMS
R = 1700 OHMS
R = 1300 OHMS
ATTENUATION
FREQUENCY - CPS

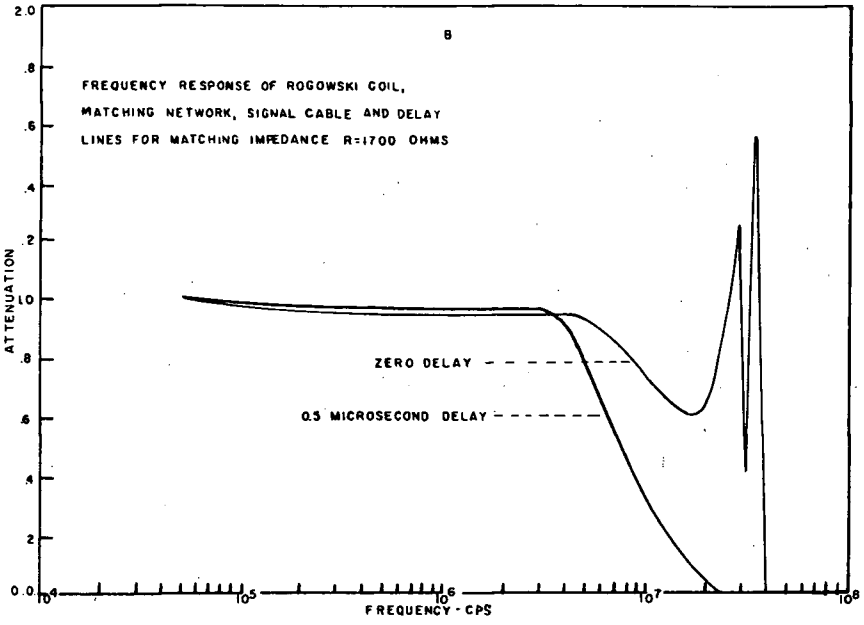
B
FREQUENCY RESPONSE OF ROGOWSKI COIL, MATCHING NETWORK, SIGNAL CABLE AND DELAY LINES FOR MATCHING IMPEDANCE R=1700 OHMS
ZERO DELAY
0.5 MICROSECOND DELAY
ATTENUATION
FREQUENCY - CPS

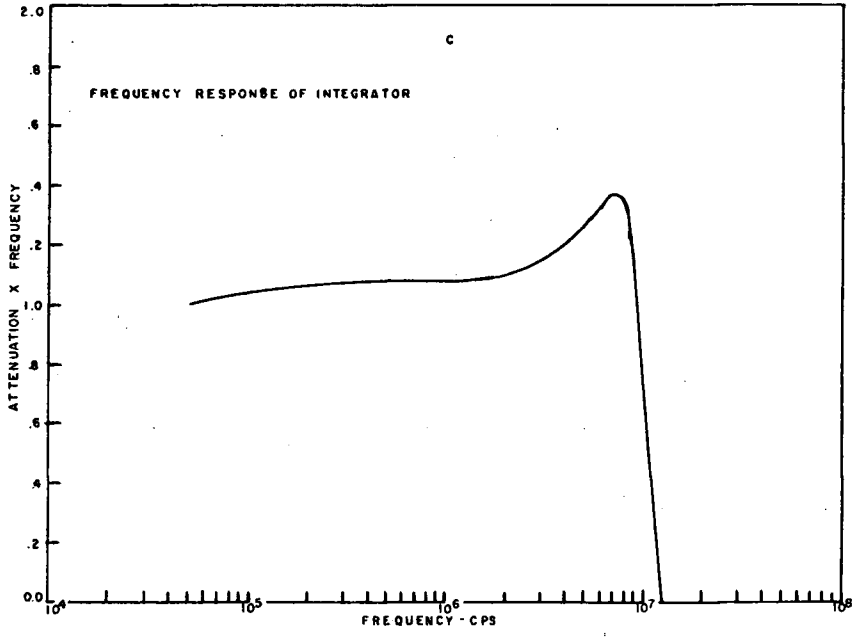
C
FREQUENCY RESPONSE OF INTEGRATOR
ATTENUATION X FREQUENCY
FREQUENCY - CPS

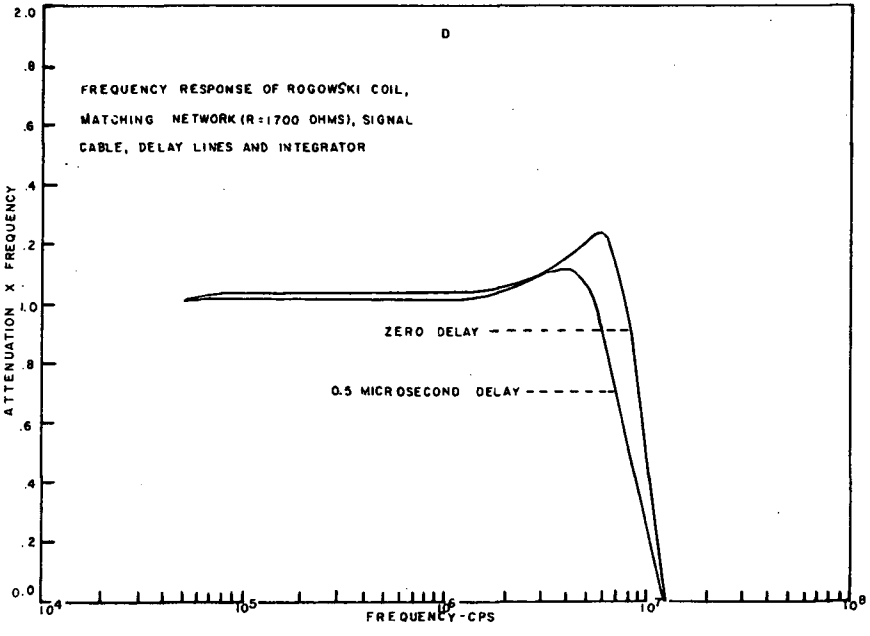
D
FREQUENCY RESPONSE OF ROGOWSKI COIL, MATCHING NETWORK (R=1700 OHMS), SIGNAL CABLE, DELAY LINES AND INTEGRATOR
ZERO DELAY
0.5 MICROSECOND DELAY
ATTENUATION X FREQUENCY
FREQUENCY - CPS

concerned (see page 33).

The results of the frequency response measurements carried out in the manner described above are presented in figure 13, page 33. The attentuation for the various circuits mentioned above has been normalized to unity at 0.05 Mc/s in all cases and plotted against frequency.

To conclude this subsection, the results of the frequency response measurements are presented in tabular form in figure 14.

CIRCUIT	COMPONENTS OF CIRCUIT	RESPONSE
$\frac{dI}{dt}$ measuring circuit a)	Rogowski coil; matching network (R_m,R_T); signal cable	Flat to 4 Mc/s; 3 db down at 12 Mc/s
$\frac{dI}{dt}$ measuring circuit with delay b)	Rogowski coil; matching network (R_m,R_T); signal cable; delay lines	Flat to 3Mc/s; 3 db down at 6 Mc/s
Current (I) measuring circuit (also called Rogowski coil measuring circuit) c)	Rogowski coil; matching network (R_m,R_T), signal cable; integrating network	Flat to 5 Mc/s; 3 db down at 9 Mc/s
Current (I) measuring circuit with delay (also called Rogowski coil measuring circuit with delay) d)	Rogowski coil; matching network (R_m,R_T); signal cable; integrating network; delay line	Flat to 5 Mc/s; 3 db down at 7 Mc/s

Figure 14: Resumé of Frequency Response Measurements

The dI/dt measuring circuit (a of figure 14, page 34) with $R_m = 800$ ohms is used extensively in the noise investigation because this circuit has the greatest bandwidth available.

3.5 CURRENT SENSITIVITY

The output signal (V_o) from the integrator of the circuit of figure 10, page 24, can be expressed in terms of the discharge current (I) through the following considerations.

At the output of the Rogowski coil (see page 21)

$$V_c = -2.1 \times 10^{-8} \frac{dI}{dt} \text{ volts}$$

Inverting the transform of the transfer function for the normal measuring circuit (see page 27)

$$V_o = \frac{R_T}{R_T + 2R_m} \cdot \frac{1}{R_i C_i} \cdot V_c \text{ volts}$$

Combining these expressions yields

$$V_o = -2.1 \times 10^{-8} \frac{R_T}{R_T + 2R_m} \cdot \frac{1}{R_i C_i} \cdot I \text{ volts}$$

Substituting the values quoted in figure 10, page 24, for the parameters in the above equation yields

$$V_o = -\frac{I}{4.3 \times 10^4} \text{ volts}$$

Thus the current sensitivity is 4.3×10^4 amps. per volt. From the current waveform shown in the upper trace of figure 15, page 37, the maximum current which flows in the discharge circuit is 1.1×10^3 amp and this peak is attained in 2.4×10^{-6} sec. This gives an approximate value for dI/dt of 0.5×10^{11} which is in agreement with the value of 10^{11} used in subsection 3.1, page 20.

The current sensitivity of the measuring circuit may be obtained experimentally as follows. The total charge on the capacitor bank can be calculated from the known value of the initial voltage on the bank and its capacitance. This charge is equated to the integral of the current waveform - an integral most accurately evaluated by numerical integration. The ratio of the charge to the area under the current waveform (in units of volts · seconds) yields a scaling factor which relates the magnitude of the discharge current to the output voltage of the measuring circuit.

The current sensitivity for a circuit which differs from that of figure 10, page 24, only in the value of R_m has been determined by my colleague C. C. Daughney using both methods presented above. The two values of the current sensitivity obtained in this way agreed to within 5%.

4.0 INVESTIGATION OF NOISE SIGNAL

The investigation presented in this subsection is concerned with the noise signal accompanying current measurements being made on a pulsed discharge circuit by means of a Rogowski coil. Oscilloscope traces obtained using the Rogowski coil measuring circuit of figure 10, page 24, and a Type 545 A Tektronix oscilloscope with Type G differential preamplifier are shown in figure 15.

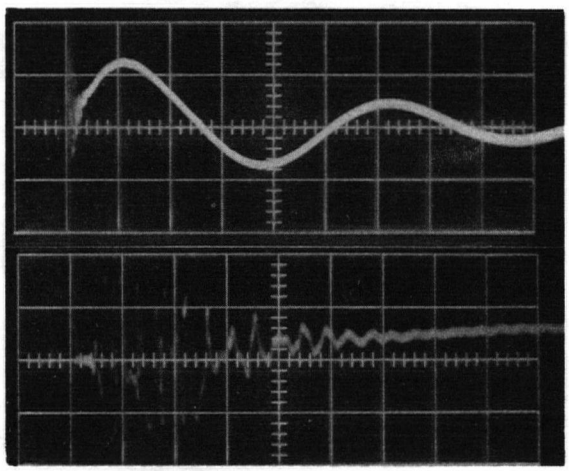

Figure 15: Current Waveform and Noise Signal

Upper trace: 2 v/cm vertical, 2 μsec/cm horizontal; current waveform from Rogowski coil.

Lower trace: 10/3 v/cm vertical; 0.2 μsec horizontal; noise signal at initial rise of current waveform from Rogowski coil.

The upper trace of figure 15 is a current waveform; that is, the amplitude of this trace is directly proportional to the magnitude of the current which flows in the discharge circuit after the discharge is fired. It is noted that the initial time and rate at which the

discharge current rises is obscured by a noise signal. This noise signal is shown with the time scale expanded in the lower trace of figure 15.

The noise signal mentioned above has a characteristic shape. For the initial 0.5 μ sec, the noise signal appears to consist of a superposition of several signals varying in frequency from 10 Mc/s to about 40 Mc/s. During the next 0.5 μ sec interval, the amplitude of the signal has fallen by a factor of 5 and only a 15 Mc/s signal remains.

As has been mentioned on page 2, the noise signal under investigation may be a genuine noise signal induced in the Rogowski coil by fluctuations in the discharge current or a spurious noise signal due to stray coupling between the measuring and discharge circuits or a combination thereof.

The discussion which follows deals with the manner in which the sources of the noise signal were determined and the method by which the noise signal can be eliminated from the current waveform.

4.1 GROUNDING

As mentioned on page 9, the trigger generator prevents grounding of the discharge circuit through the triggering electronics. In this way, an undesirable ground loop is eliminated from the discharge circuit. A second ground loop exists through the high voltage power supply as can be seen from figure 3, page 6. However, no change in the noise signal is observed when the mains and ground of the power supply are removed before firing the discharge apparatus.

Capacitative coupling between the Rogowski coil and the discharge circuit is reduced considerably when the discharge circuit is grounded

near the coil instead of at the capacitor bank. This procedure minimizes the effect on the measuring circuit of the oscillating potential difference across the discharge vessel (see page 21).

Considering the options of simple grounding connections, the following connections tend to minimize the noise signal:

a) grounding the discharge circuit at the top of the discharge vessel near the coil;

b) earthing the brass shielding can of the Rogowski coil at the main ground of the discharge circuit;

c) allowing the oscilloscope to float - grounded neither through the power outlet nor at the main ground of the discharge circuit.

With respect to c) the best arrangement of the power cord of the oscilloscope is to connect the safety ground of the cord at the power outlet but not at the oscilloscope.

In general, grounding connections were found to be ineffective for frequencies greater than 15 Mc/s, particularly near the discharge apparatus where the radiation field is largest.

4.2 RADIATIVE COUPLING

Figure 16 represents the Rogowski coil separated from the upper electrode of the discharge vessel by a grounded brass shield (see page 18) and illustrates a case of capacitative coupling of particular interest in this noise investigation.

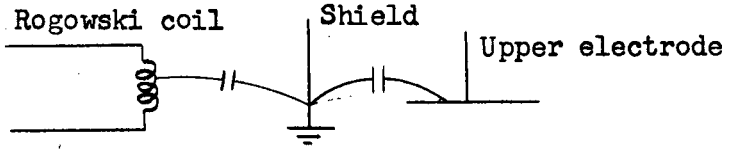

Figure 16: Example of Capacitative Coupling

Potential fluctuations on the upper electrode of the discharge vessel are imparted to the brass shield and thence to the coil by way of displacement currents as indicated by the stray capacitance drawn in figure 16. Grounding the brass shield reduces the capacitative coupling at frequencies below 15 Mc/s but at frequencies higher than this the effect of ground connections decreases due to the lead inductance while the capacitative coupling becomes increasingly efficient.

The component of the noise signal due to the source of capacitative coupling discussed above can be rejected by using a balanced measuring circuit (see page 19) feeding a balanced differential preamplifier unit in the oscilloscope. The action of the balanced measuring system requires further explanation. As mentioned on page 30, no point in the measuring system is grounded. Therefore, the potential at any point in the circuit can be chosen as a reference potential and it is convenient to choose, for this, the point midway between the output terminals of the Rogowski coil. Now the potential which appears at the output terminals of the coil is a superposition of a magnetic and a noise component. The magnetic component of the potential is induced in the Rogowski coil by the discharge current. The noise component arises from capacitative coupling between the Rogowski coil and upper electrode of the discharge vessel (see page 39). With respect to the magnetic component, the potential of one terminal of the coil is 180 degrees out of phase with the potential at the other terminal, relative to the reference potential chosen above. On the other hand, the potentials at the output terminals of the coil due to the noise component are in phase. By subtracting the signal at one terminal from the signal at the other terminal, the noise component is rejected, leaving only

the magnetic component.

The traces in figure 17 are dI/dt signals (I is the discharge current) taken using the Rogowski coil measuring circuit of figure 10, page 24, without the integrators. These traces are taken under

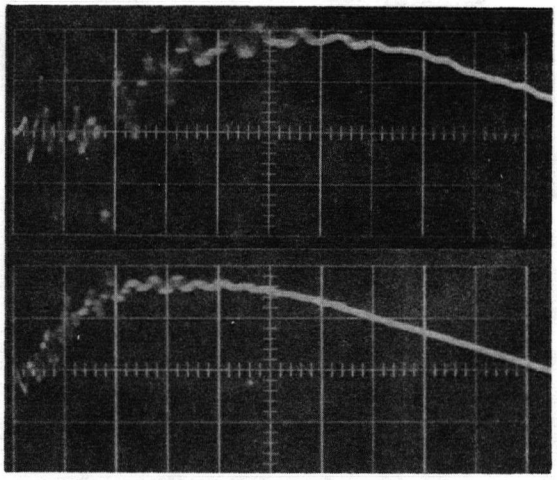

Figure 17: Effect on Noise Signal of a Completely Balanced Measuring System

Upper trace: 33 v/cm vertical; 0.2 μsec/cm horizontal; dI/dt waveform from Rogowski coil using Type K (single) preamplifier.

Lower trace: 33 v/cm vertical; 0.2 μsec/cm horizontal; dI/dt waveform from Rogowski coil using Type G (differential) preamplifier.

idential experimental conditions except that with the oscilloscope a Tektronix Type K single input preamplifier was used for obtaining the upper trace while a Tektronix Type G differential preamplifier was used for obtaining the lower trace. The result is that the amplitude

of the noise signal accompanying the dI/dt waveform is reduced by a factor of about two when a completely balanced measuring system is used. The time base of the lower trace is shifted relative to that of the upper trace due to rejection of the noise signal prior to the rise of the dI/dt signal by the differential preamplifier.

There exist several sources of capacitative coupling between the measuring and discharge circuits other than the one discussed above. For example, the fluctuating electric fields produced by the discharge circuit may be picked up on the chassis of the oscilloscope. In connection with this example, the next paragraph will be used to discuss an experiment which demonstrates that the mode by which the oscilloscope sweep is triggered plays an important role in the reduction of the noise signal appearing on the current waveform.

The triggering mode of the oscilloscope was set to "external" and all input connections to the oscilloscope were removed except for an aerial which was inserted into the external trigger input terminal. The aerial consisted of a 6" straight length of flame seal wire. The discharge circuit was then fired in the normal manner (see page 4) and a trace was observed when the aerial was connected but not when the aerial was removed. This shows that a signal enters the scope by means of the aerial. The signal obtained in the above manner is shown in the upper trace of figure 18, page 43. When the attenuation of the preamplifier unit of the oscilloscope was altered, the amplitude of the above mentioned signal remained unchanged. This means that if any signal enters the oscilloscope through the preamplifier input terminals, its amplitude must be small compared with the amplitude of the signal

shown in the upper trace of figure 18. The conclusion to be drawn is that the trigger input terminal of the oscilloscope is not isolated from the vertical deflection system of the oscilloscope and any connections to this terminal may be a possible source of noise signals. This conclusion is confirmed by the current waveforms shown in the middle and lower traces of figure 18. These traces were taken under identical experimental conditions except that for the middle trace the oscilloscope sweep was triggered externally using an aerial similar to the one described above, while for the lower trace the sweep was triggered internally. Thus the amplitude of the noise signal accompanying the current waveform is reduced by a factor of about three when internal triggering is used instead of external triggering.

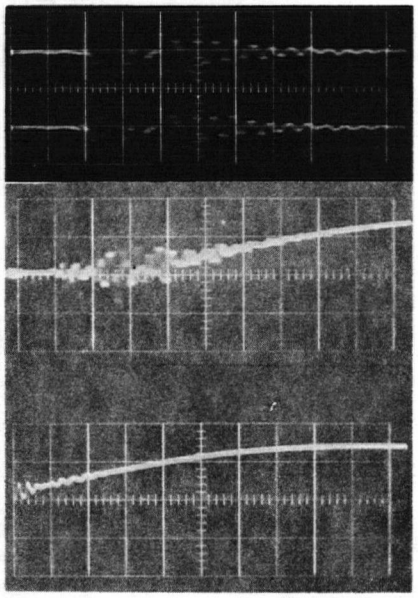

Figure 18: Effect on Noise Signal of Internal Triggering

All traces: 1 v/cm vertical, 0.2 μsec/cm horizontal.

Upper trace: Noise signal with no input connections to oscilloscope (amplitude independent of preamplifier attenuation).

Middle trace: Current waveform from Rogowski coil using external triggering mode.

Lower trace: Current waveform from Rogowski coil using internal triggering mode.

Triggering internally, while yielding a significant reduction in the amplitude of the noise signal, requires a delicate adjustment of the stability and triggering level controls of the oscilloscope. For oscilloscopes of the type used in this investigation (Tektronix 545 A) the adjustment is achieved as follows: rotate the trigger level indicator fully in either the positive or negative direction depending, respectively, on whether positive or negative internal triggering is used. Rotate the stability control clockwise as far as possible so that the single sweep reset just holds. Next, rotate the triggering level control toward zero until the sweep is triggered. Back off the triggering level control about 2 degrees. This should complete the adjustment of the oscilloscope triggering but finer adjustment of the triggering level control may still be required.

As can be seen from the lower trace of figure 18, page 43, a noise signal remains on the current waveform even when the oscilloscope sweep is triggered internally. It turns out that the amplitude of this noise signal increases as the preamplifier attenuation is decreased, which means that this noise signal must enter the oscilloscope through the preamplifier input terminals. Possibly this signal is a genuine signal produced by fluctuations in the discharge current. On the other hand, the signal may be due to fluctuations of the potential of the oscilloscope chassis caused by pick up of electromagnetic signals radiated by the discharge circuit. If the latter case is true, then the amplitude of the noise signal which remains when internal triggering is used should decrease as the distance separating the oscilloscope from the discharge circuit is increased.

The current waveforms shown in figure 19 were taken with the sweep of the oscilloscope triggered internally. For both traces the same length of signal cable was used, but the distance separating the oscilloscope from the discharge apparatus was 5 feet for the upper trace and 25 feet for the lower trace. The amplitude of the noise signal in the lower trace is less than half that in the upper trace. The conclusion to be drawn from this result is that the noise signal which remains on the current waveform when using internal triggering is due to electromagnetic signals radiated by the discharge apparatus. These signals enter the oscilloscope by capacitative and inductive pickup on its chassis.

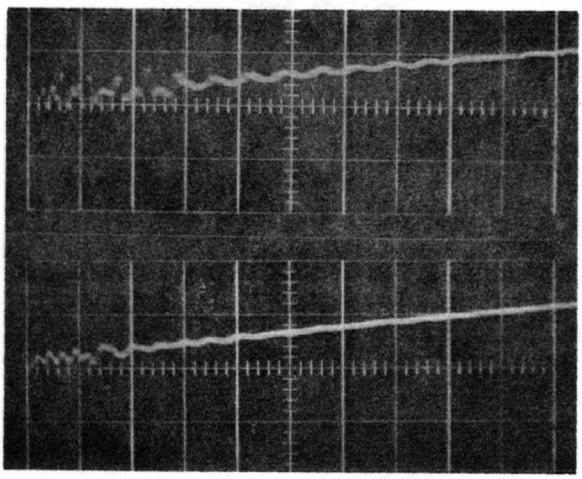

Figure 19: Effect on Noise Signal of Distance Separating Discharge Circuit and Oscilloscope

Both traces: 1 v/cm vertical, 0.1 μsec horizontal; current waveforms from Rogowski coil with oscilloscope sweep triggered internally.

Upper trace: Oscilloscope 5 feet from discharge circuit.

Lower trace: Oscilloscope 25 feet from discharge circuit.

It is inconvenient, however, to have the oscilloscope separated from the discharge apparatus by those distances necessary to reduce the amplitude of the noise signal appreciably. A more satisfactory arrangement is to isolate the oscilloscope from the radiation field of the discharge apparatus by enclosing the oscilloscope in a Faraday cage. The cage (a photograph of which is shown in Appendix II, page 61) consists of 1/8 inch brass mesh wrapped on a Dexion framework.

The dI/dt waveforms shown in figure 20 illustrate the effect of the Faraday cage on the noise signal. Both traces were taken under the same experimental conditions except that for the lower trace the oscilloscope was enclosed in the Faraday cage described above while for the upper

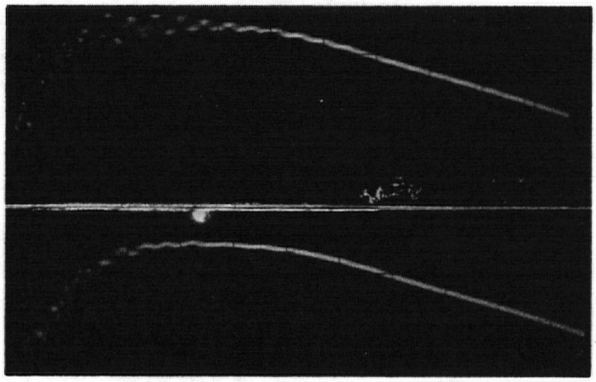

Figure 20: Effect on Noise Signal of Faraday Cage

Both traces: 33 v/cm vertical, 0.2 μsec horizontal; dI/dt waveform from Rogowski coil using internal triggering.

Upper trace: Oscilloscope removed from Faraday cage.

Lower trace: Oscilloscope enclosed in Faraday cage.

trace the cage was removed. In taking the lower trace, the Faraday cage was grounded to an earthing rod but not the same earthing rod at which the discharge circuit was grounded. The amplitude of the noise signal obtained using the cage is several times smaller than the signal obtained not using the cage, so that clearly the cage is effective in suppressing the noise signal.

So far three means by which spurious signals generated by the discharge circuit enter the oscilloscope have been discussed; namely, capacitative coupling to the Rogowski coil, the triggering mode of the oscilloscope sweep and radiative pick up on the chassis of the oscilloscope. Yet another path remains to be discussed.

Conceivably, electromagnetic signals radiated by the discharge circuit are picked up on the nearby a.c. power lines and enter the oscilloscope via its power cord. In view of this, an isolated power supply for the oscilloscope was constructed, which consisted of a 3-phase motor driving a 400 cps generator. The motor and generator were connected by a fibre belt and the generator was enclosed in an aluminium container which was then grounded to an earthing rod. The amplitude of the noise signal obtained using the isolated power supply for the oscilloscope turned out to be greater than the amplitude of the signal obtained when a.c. supply from the power mains was used. This simply means that radiative pick up by the isolated power supply is greater than any noise signal which might be coming along the a.c. mains.

A second isolated power supply was used in the form of a battery powered transistorized oscilloscope (Tektronix Type 321). In this case the signal obtained when the oscilloscope was powered from the a.c.

mains was noisier than the signal obtained when the battery supply was used. Thus noise signals generated by the discharge circuit are picked up on the a.c. power lines supplying the oscilloscope and enter the oscilloscope through the power cord.

Up to this point, all of the results have indicated that the noise signal remaining on the current waveform after using a balanced measuring circuit and differential preamplifier is due to signals radiated from the discharge circuit. In view of this, it is reasonable to try delaying the signal from the measuring circuit before displaying it on the oscilloscope so that the signal from the measuring circuit will appear after the normal noise signal has died away.

Two General Radio Type 314-S86 variable delay lines, each providing a maximum delay of 0.5 μ sec, were connected in parallel as shown in figure 21. This unit was inserted between the signal cable and integrating network of figure 10, page 24. (The delay line of figure 21 has also

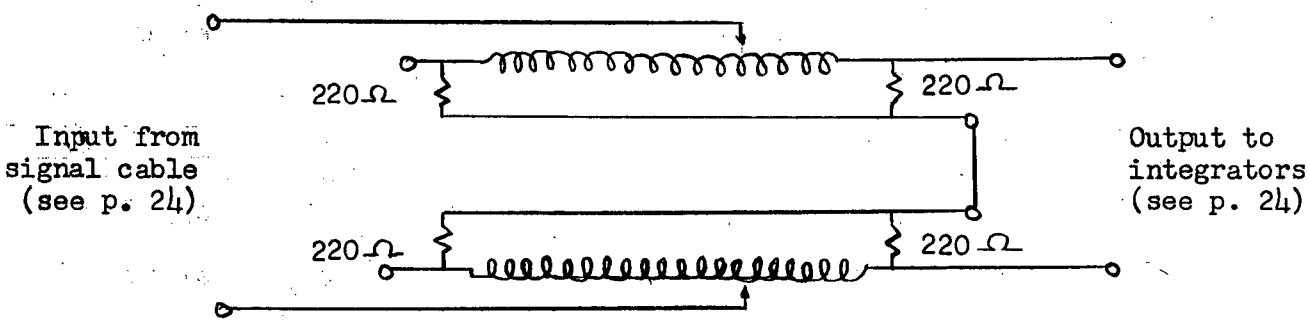

Figure 21: Variable Delay Line

been discussed on page 30). The current waveforms obtained using the Rogowski coil measuring circuit with delay lines and external triggering from an aerial (see page 42) are shown in figure 22. The upper trace is undelayed while the lower trace is delayed by 0.5 μ sec. For the lower trace, the Rogowski coil signal is clean and rises 0.5 μ sec after the normal noise signal.

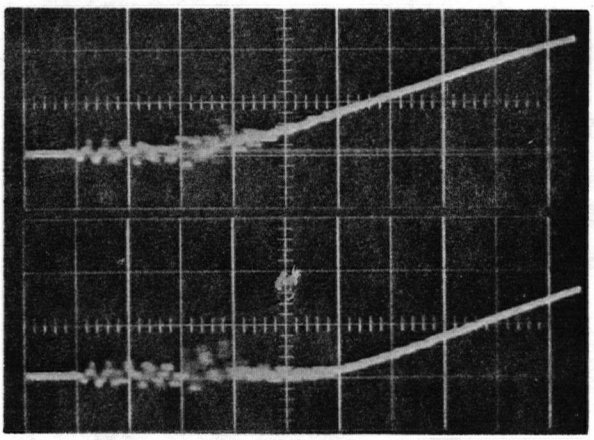

Figure 22: Effect on Noise Signal of Delaying Current Waveform

Both traces: 1 v/cm vertical, 0.2 μ sec horizontal; current waveform from Rogowski coil using external triggering.

Upper trace: Undelayed current waveform.

Lower trace: Current waveform delayed by 0.5 μ sec.

The traces shown in figure 23, page 50, are dI/dt waveforms taken using that Rogowski coil measuring circuit which possesses the widest bandpass available in this investigation. This circuit consists of the Rogowski coil with matching impedance $R = R_T + 2\ R_m$ of 1700 ohms, signal cable terminated in its characteristic impedance of $R_T = 100$ ohms (see page 24) and delay line which has been properly terminated (see

page 30). The frequency response of this circuit with zero delay is flat to 4 Mc/s and 3 db down at 12 Mc/s and with full delay (0.5 μsec) is flat to 3 Mc/s and 3 db down at 6 Mc/s (see page 34). In taking the traces, the discharge circuit was fired in the normal manner (see page 4) and the sweep of the oscilloscope was triggered externally from an aerial (see page 42).

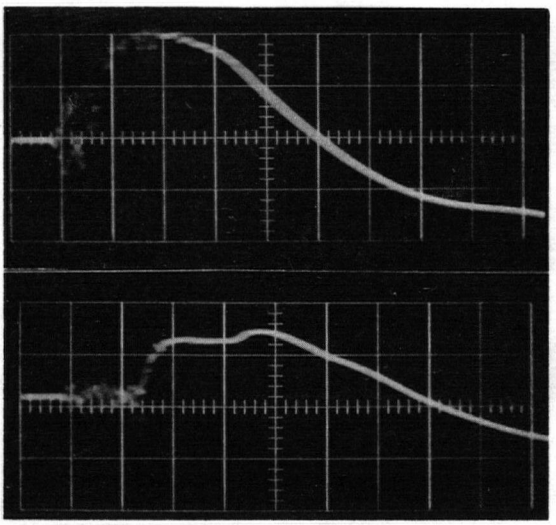

Figure 23: Delayed dI/dt Waveform

Both traces: 5 v/cm vertical, 0.3 μsec/cm horizontal; dI/dt waveforms from Rogowski coil using external triggering.

Upper trace: Undelayed dI/dt waveform.

Lower trace: dI/dt waveform delayed by 0.5 μsec.

Once again, the delayed waveform is clean and rises 0.5 μsec after the normal noise signal. This result means that the noise signal under investigation is not produced by fluctuations of the

discharge current. Otherwise, the noise signal would be delayed along with the dI/dt waveform and appear during the initial rise of the dI/dt waveform instead of prior to its rise.

The current waveforms in figure 24 are presented in order to show the effect on the noise signal of combining all the features discussed in this subsection which help to produce a clean current waveform. The most important features are: 1) a balanced Rogowski coil measuring circuit feeding a differential preamplifier, 2) triggering the oscilloscope sweep internally, 3) isolation of the oscilloscope from the radiation field of the discharge circuit by means of a Faraday cage and 4) delaying the signal from the Rogowski coil by 0.5 μ sec before displaying it on the oscilloscope.

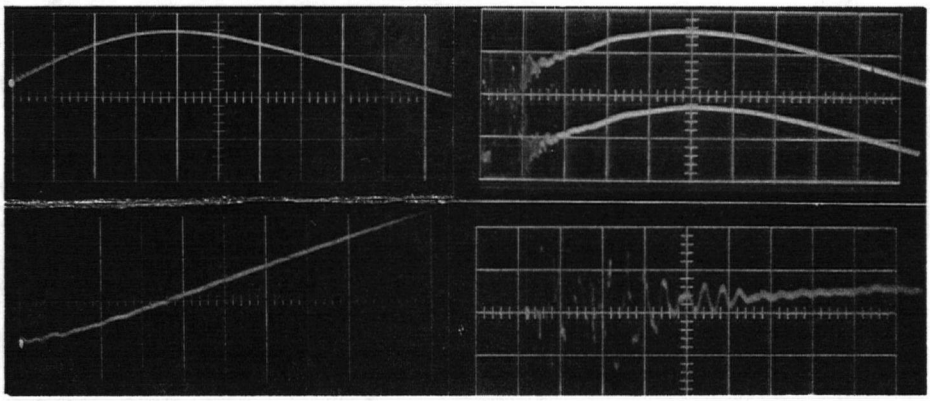

Figure 24: Effect on Noise Signal of Combined Noise Reducing Features

Left traces: Current waveforms from Rogowski coil incorporating all noise reducing features discussed in this subsection.

Right traces: Current waveforms from Rogowski coil incorporating none of the noise reducing features discussed in this subsection.

Upper left trace: 2 v/cm vertical, 0.5 μsec/cm horizontal.
Upper right trace: 2 v/cm vertical, 0.5 μsec/cm horizontal.
Lower left trace: 0.5 v/cm vertical, 0.1 μsec/cm horizontal.
Lower right trace: 10/3 v/cm vertical, 0.2 μsec/cm horizontal.

The results of this subsection can be summarized in the following way. The noise signal accompanying current measurements is not induced in the Rogowski coil by fluctuations of the discharge current but arises due to stray coupling between the measuring and discharge circuits. Part of the noise signal enters the measuring system by way of capacitative coupling between the Rogowski coil and upper electrode of the discharge vessel. This portion of the noise signal is removed from the current waveform by using a balanced Rogowski coil measuring circuit feeding a differential preamplifier. The remainder of the noise signal enters the measuring system by way of radiative coupling between the discharge apparatus and the chassis of the oscilloscope and the power mains which supply the oscilloscope. This portion of the noise signal is removed by delaying the signal from the Rogowski coil by 0.5 μsec (that is, until the noise signal radiated by the discharge circuit has died away). The current waveform obtained in this way is clean and rises 0.5 μsec after the normal noise signal.

4.3 NOISE SOURCES

This subsection deals with the investigation of the sources of the noise signal which has been discussed in the previous subsection.

It is conceivable that the noise signal in question arises due to relaxation processes in the discharge vessel and spark gap switches of the discharge apparatus. The term "relaxation process" will be explained below by way of an example.

The circuit shown in figure 25, page 53, represents a simplified discharge circuit. Suppose that the spark gap switch has just entered

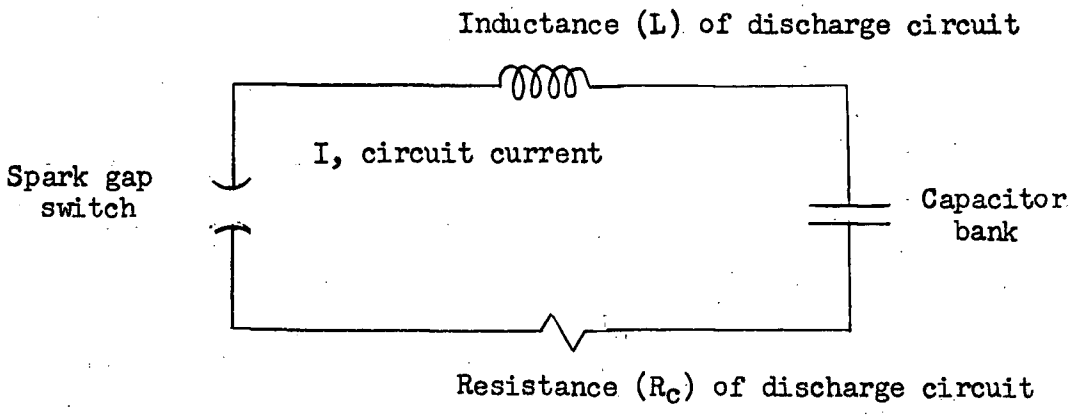

Figure 25: Simplified Discharge Circuit

the conducting state. If the circuit resistance (R_c) is sufficiently small, the circuit current (I) will rise at a rate which will produce a potential drop across the circuit inductance (L) which is sufficient to cause the potential difference across the spark gap to drop below the value necessary to maintain the switch in the conducting state. The spark gap will then "relax" into the nonconducting state. However, as this relaxation occurs, the current (I) tends to zero and so does the potential drop across the circuit inductance (L). As a result, the potential difference across the spark gap rises until the gap again breaks down (provided, of course, that, during the relaxation cycle, the potential of the capacitor bank has not fallen below the breakdown potential of the spark gap switch). The circuit is thus back to the initially assumed state and the process begins to repeat itself. This cycle is referred to as a "relaxation process".

In connection with the above example, consider the following order of magnitude calculation for the discharge circuit used in this investigation. If only the impedance of the discharge circuit due to its

inductance (L) is taken into account, the current (I) necessary to produce a potential drop across the inductance (L) equal to 1/2 the potential of the condenser bank (V_B, say) is

$$I = \frac{\frac{1}{2} V_B}{wL} \text{ amps}$$

where w is the (angular) frequency of the relaxation process. From page 17, the total inductance (L) of the discharge circuit is 150 nH. The condenser bank is normally fired at $V_B \simeq 12$ kV. If we suppose that the relaxation process described above occurs at a frequency of 20 Mc/s (frequencies of this order are present in the noise signal shown in the lower trace of figure 15, page 37), then

$$I = \frac{\frac{1}{2} \cdot 12 \times 10^3}{6.28 \times 20 \times 10^6 \times 150 \times 10^{-9}}$$

$$\sim 300 \text{ amps}$$

Since peak currents in the discharge circuit are the order of 10^5 amps (see page 36), current fluctuations of 10^2 amps at the initial rise of the discharge current are reasonable. The above calculation, therefore, shows that it is possible for relaxation processes in the discharge vessel and spark gap switches of the discharge circuit to be responsible for production of the noise signals in the megacycle range.

However, the anticipated amplitude of the current fluctuations is too small to be observed using the Rogowski coil system. In order to demonstrate this, consider the upper and lower left traces shown in figure 24, page 51. The lower left trace attains an amplitude of about

4 centimeters on the graticule in 1 μsec and therefore represents a current whose maximum value is about 1/2 the peak current (see upper left trace) in the discharge circuit (i.e. $\sim 10^3$ amps as noted on page 54).

To produce fluctuation in the trace of 0.1 cm in amplitude, a fluctuation in the discharge current of $\frac{0.1 \text{ cm}}{4 \text{ cm}} \times \frac{1}{2} \times 10^5 \text{ amp} = 10^3 \text{ amp}$ is required.

It is highly likely, however, that the very large fluctuations in potential (of the order $V_B/2$ or 6 kV) will be coupled spuriously to the measuring system to produce a noise signal of about one volt in amplitude. In view of this it is reasonable to investigate the production of noise signals in the discharge vessel and spark gap switches by altering the breakdown conditions in these devices.

To discover if the noise signal depends on the breakdown conditions in the discharge vessel, an experiment was performed which consisted of filling the discharge vessel, in turn, with argon, nitrogen, hydrogen, oxygen and air over a pressure range from 100 to 2000 μ Hg. However, no significant change in either the amplitude or frequency of the noise signal was observed when current measurements were made in the normal way. Thus the noise signal associated with current measurement using a Rogowski coil apparently does not depend on breakdown conditions in the discharge vessel.

To investigate the noise produced by the main spark gap switch (S_2 on page 6), the spark gap chamber of this switch was pressurized with commercial argon. The traces shown in figure 26, page 56, are dI/dt waveforms which were taken by charging the condenser bank to 12 kV and firing the discharge circuit in the normal manner. However, for the

upper trace of figure 26 the spark gap chamber contained air at atmospheric pressure while for the lower trace the chamber contained argon at 22 lbs/sq. in. The noise signal is thus largely due to the main spark gap switch and is greatly reduced by operating the spark gap switch in an argon atmosphere. (It was found, however, that pressurizing the spark gap chamber with argon has a serious disadvantage; namely, the breakdown potential of the spark gap becomes erratic).

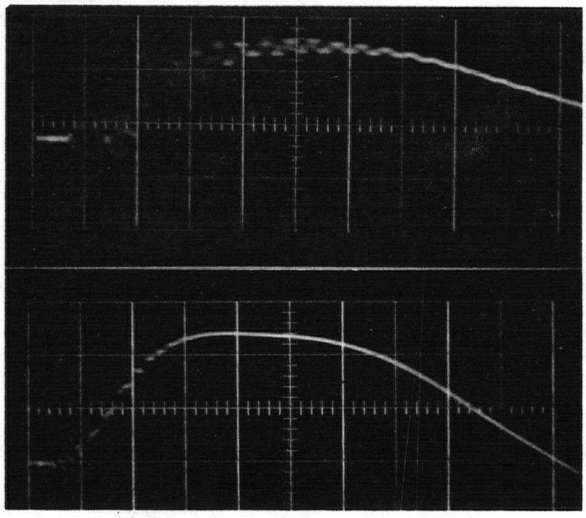

Figure 26: Noise Signal from Main Spark Gap Switch

Upper trace: 33 v/cm vertical, 0.2 μsec/cm horizontal; dI/dt waveform from Rogowski coil taken operating main spark gap switch in open air.

Lower trace: 33 v/cm vertical, 0.3 μsec/cm horizontal; dI/dt waveform from Rogowski coil taken operating the main spark gap switch in argon at 22 lbs./sq.in.

In connection with noise signals produced by spark gap switches, Curzon and Daughney (1963) claim that such noise signals can be overcome

by suitable design of the electrode system of the spark gap switch. Attempts by the author to duplicate their results has met with only partial success in that while noise free breakdown of the spark gap switch, under conditions specified by them, was observed occasionally, the effect was not reproducible.

It was found that only one other significant source of noise exists in the discharge circuit; namely, the trigger generator. The signal shown in figure 27 was obtained by overvolting the trigger generator spark gap (S_1 of figure 3, page 6) but not allowing the main spark gap switch to break down. The 15 Mc/s frequency which dominates this signal is simply the natural ringing frequency $\left(\omega = \frac{1}{\sqrt{LC}}\right)$ of the trigger generator circuit (see page 13).

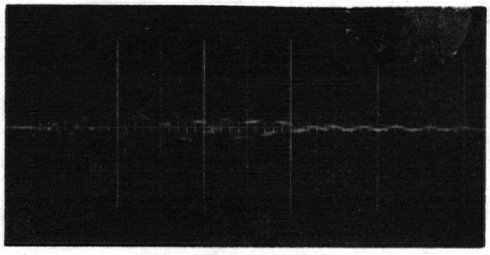

Figure 27: Noise Signal Produced by Trigger Generator

Time base: 0.1 μ sec/cm.

In conclusion, the important results of this subsection are that 1) the principal source of noise in the discharge apparatus is the main spark gap switch - the noise from this switch is greatly reduced by operating it in an argon atmosphere; and 2) the trigger generator produces a noise signal whose frequency is predominantly 15 Mc/s.

5.0 CONCLUSIONS

The Rogowski coil has been found to be an excellent device for the measurement of current in a pulsed discharge circuit, due to its favourable signal to noise ratio.

Normally, a noise signal is coincident with the initial rise of the current waveform obtained with the Rogowski coil. However, it has been shown that this signal is not the result of voltages induced in the Rogowski coil by fluctuations in the current being measured. It is, instead, a spurious noise signal which appears on the current waveform because of stray coupling between the measuring system and the discharge apparatus.

Part of the noise signal enters the measuring circuit by way of capacitative coupling between the Rogowski coil and upper electrode of the discharge vessel. (The Rogowski coil encircles this electrode.) The remainder of the noise signal is the result of radiative coupling between the chassis and power lines of the oscilloscope and the discharge apparatus.

The portion of the noise signal which is picked up capacitatively by the Rogowski coil can be eliminated by using a balanced measuring circuit feeding a balanced differential preamplifier. The rest of the noise signal can be separated from the current waveform by delaying the signal from the Rogowski coil until the noise signal produced by the discharge apparatus has died away. A delay of 0.5 μsec was found to be sufficient for this purpose.

The trace shown in figure 28, page 59, is a current waveform obtained with a Rogowski coil measuring circuit incorporating the above

mentioned features. The current waveform rises cleanly 0.5 μsec after the appearance of the noise signal.

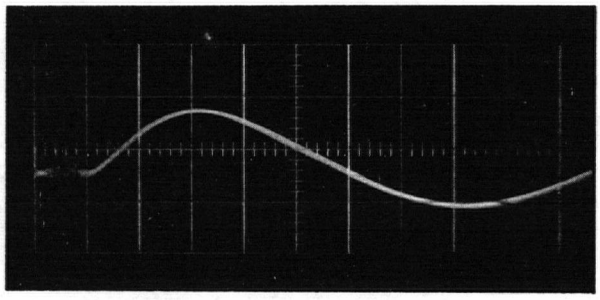

Figure 28: Clean Current Waveform

Current waveform obtained by delaying signal from balanced Rogowski coil measuring system 0.5 μ sec before displaying on oscilloscope: 2 v/cm vertical, 1 μsec/cm horizontal.

Most of the noise signal in question is produced by the spark gap switch of the main condenser bank. The trigger generator, however, produces a 15 Mc/s noise signal due to natural ringing after the generator is triggered. This result agrees with the explanation of Curzon and Daughney (1963) where the noise signal coincident with the initial rise of the discharge current is attributed to noise generated by the spark gap switch of the discharge circuit.

The noise signal generated by the main spark gap switch is greatly reduced in amplitude by operating the spark gap in an argon atmosphere. However, this has a disadvantage in that the breakdown potential of the spark gap becomes erratic.

The investigation presented in this thesis can be extended in two ways. Firstly, the design of the trigger generator can be improved in

order to eliminate noise signals produced by natural ringing in the circuit and secondly, the effect on the noise signal of various breakdown conditions in the main spark gap switch should be investigated.

APPENDIX 1. PHOTOGRAPHS OF APPARATUS

All of the apparatus used in the noise investigation has been described in the main body of the thesis (see page 4), except for the high voltage power supply (F) of figure 3, page 6. For completeness, the circuit diagram for the power supply is included here. Also, some photographs of the discharge apparatus and measuring system are presented.

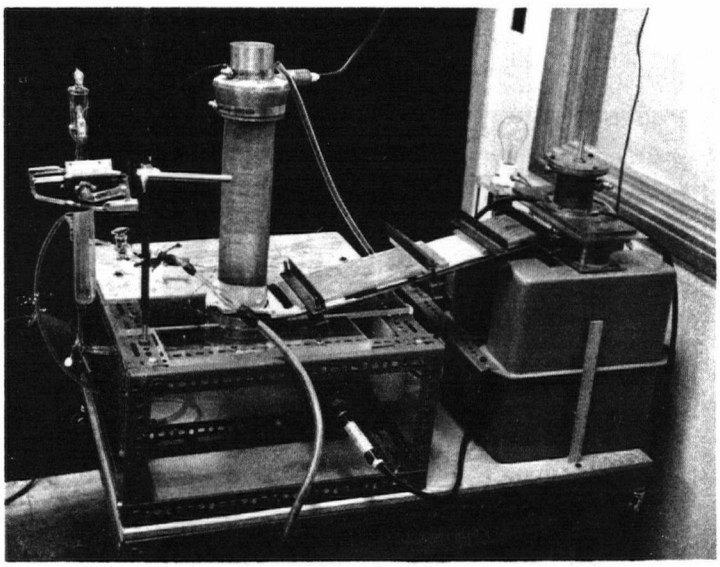

Figure 29: Photograph of Discharge Apparatus

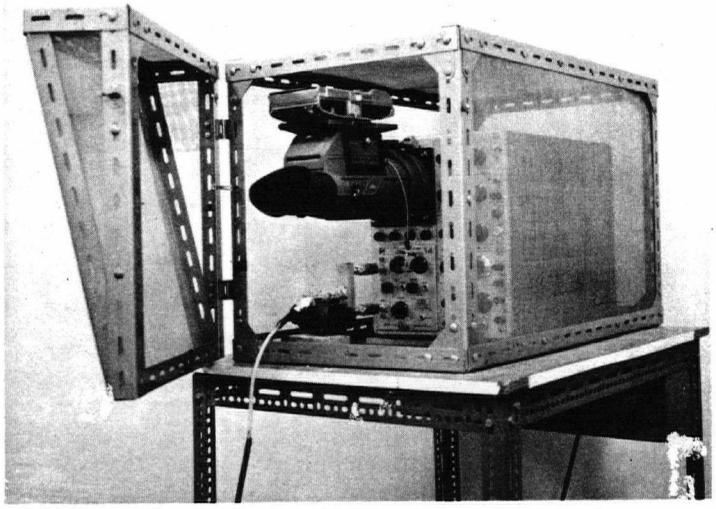

Figure 30: Photograph of Faraday Cage

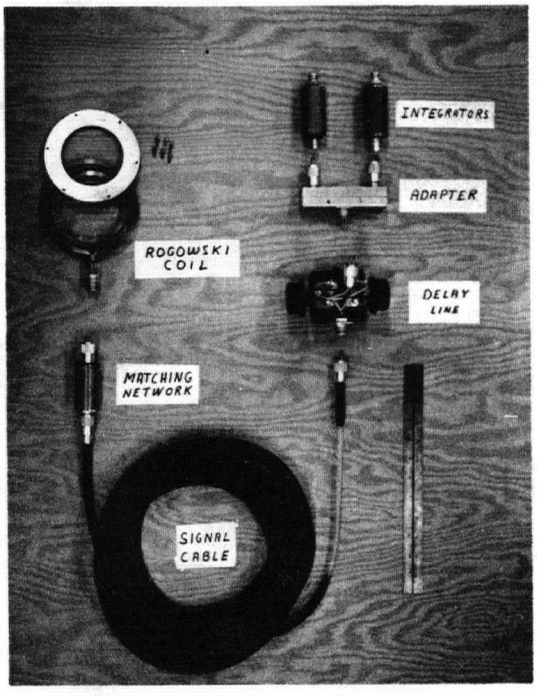

Figure 31: Photograph of Measuring Circuit

It has been found that the frequency response of the integrator is strongly influenced by the manner in which the components of the integrator are connected. In order to obtain an integrator which has the frequency response shown in curve c) on page 33, it is important that the leads which join the components of the integrator be kept as short as possible. Also, the leads should be squeezed together in order to minimize the area of the loops formed by the leads. The integrator which was used in obtaining the frequency response curve c) on page 33 is shown below. The capacitor which was used in the integrator is manufactured by Cornell Dubilier.

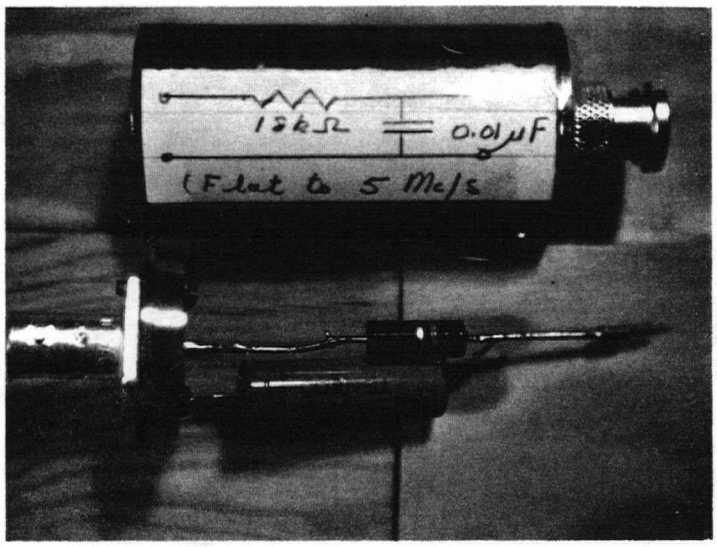

Figure 32: Photograph of Integrating Network

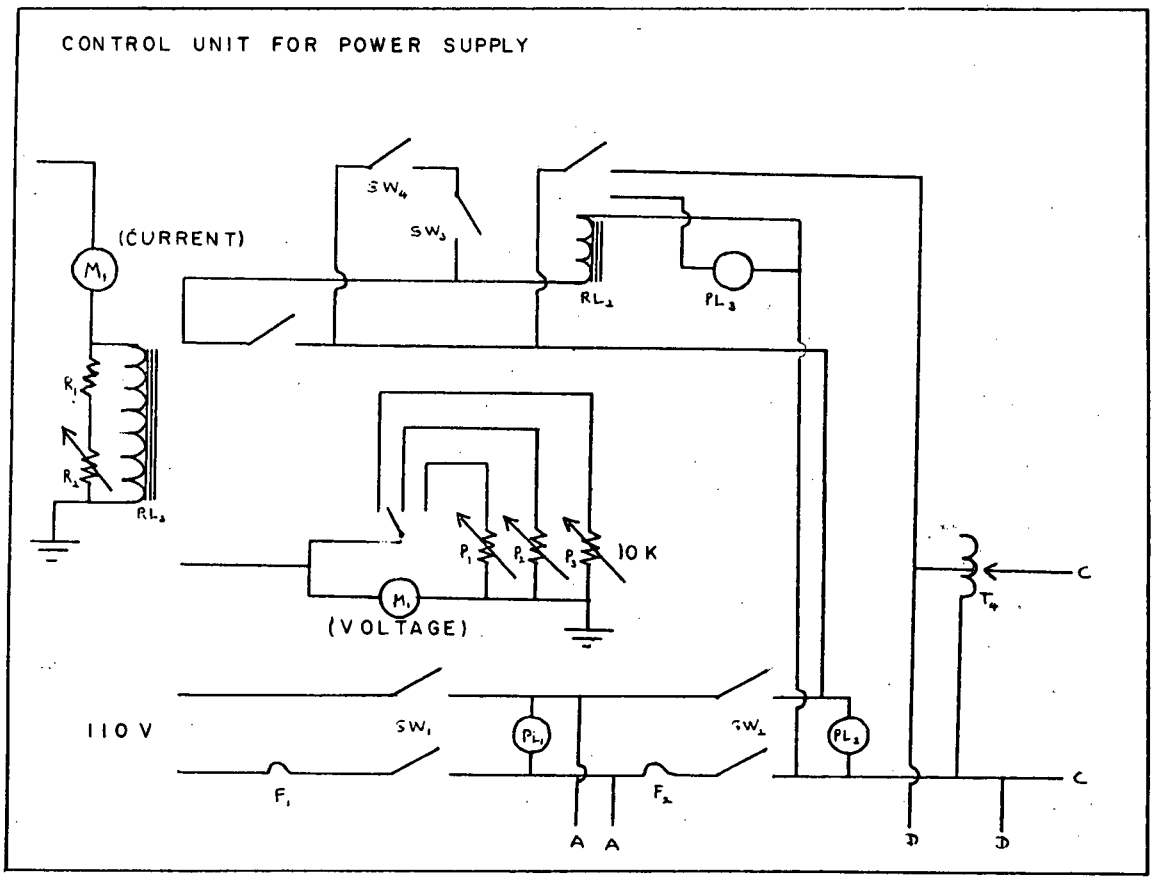

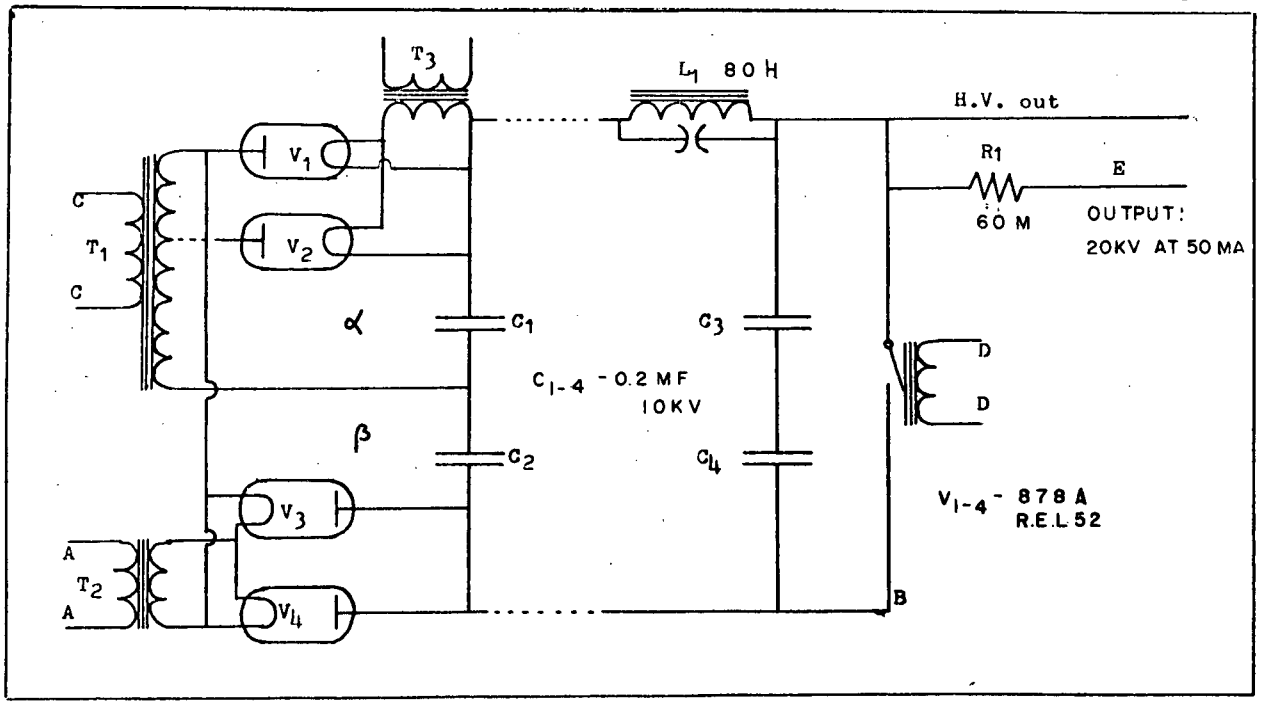

20 KV POWER SUPPLY

APPENDIX 2. FREQUENCY RESPONSE DATA

The data used in slotting the frequency response curves of figure 13, page 33, are presented below. "R" denotes the impedance which is presented to the output terminals of the Rogowski coil.

a) Rogowski coil with matching network and signal cable

R = 1300 ohms		R = 1700 ohms		R = 2100 ohms	
f (Mc/s)	Attenuation (Normalized)	f (Mc/s)	Attenuation (Normalized)	f (Mc/s)	Attenuation (Normalized)
.05	1.00	.05	1.00	.05	1.00
.5	.99	.5	1.00	.5	1.00
1	.97	1	1.00	1	1.00
3	.93	2	1.04	2	1.02
6	.78	4	1.00	4	1.06
9	.66	6	.93	6	1.09
15	.54	8	.87	8	1.04
18	.57	9	.83	10	.93
20	.61	10	.80	12	.80
22	.72	15	.63	15	.68
24	.87	20	.65	20	.64
26	1.16	25	.93	25	.91
28	1.61	30	1.48	27	1.27
30	1.73	32	.52	30	1.92
32	.96	35	.15	32	.77
34	.42	40	0	35	2.00
36	.24			37	1.13
40	0			40	0

b) Frequency Response of Rogowski coil with matching network (R = 1700 ohms), signal cable and delay lines

Zero Delay		Maximum Delay (0.5 μsec)	
f (Mc/s)	Attenuation (Normalized)	f (Mc/s)	Attenuation (Normalized)
.05	1.00	.05	1.00
.5	.95	.5	.97
1	.95	1	.97
4	.95	2	.97
6	.93	3	.97
8	.84	4	.92
10	.76	5	.80
15	.63	6	.70
18	.61	7	.59
20	.63	8	.49
25	.95	10	.38
30	1.26	15	.12
32	.40	20	.08
35	1.47	25	0
37	1.32		
40	0		

c) Frequency Response of Integrator

f (Mc/s)	Attenuation x frequency (f) (Normalized)
.05	1.00
.35	1.08
.5	1.07
1	1.07
2	1.09
3	1.15
4	1.20
5	1.27
6	1.31
7	1.37
8	1.09
9	.93
10	.69
12	0

d) Frequency Response of Rogowski coil with matching network (R = 1700 ohms), signal cable, delay lines and integrator

f (Mc/s)	Attenuation x frequency (f) (Normalized)	
	Zero Delay	0.5 μsec Delay
.05	1.00	1.00
.08	1.02	1.02
.1	1.02	1.02
.2	1.02	1.02
.4	1.02	1.03
.6	1.02	1.03
.8	1.02	1.03
1	1.02	1.03
2	1.04	1.06
4	1.14	1.10
6	1.22	.92
8	.92	.53
10	.52	.26
12	0	0

The values presented in the above table (d) were obtained by normalizing the product of the ordinate of curve b) of figure 13, page 33, the ordinate of curve c) of the same figure and the frequency for each frequency listed in the table.

REFERENCES

Bodin, H.A., Newton, A.A. and Peacock, N.J. (1960), Nuclear Fusion 1, 54

Curzon, F.L. and Daughney, C.C. (1963), Rev. Sci. Inst. 34, 430

Curzon, F.L. and Smy, P.R. (1961), Rev. Sci. Inst. 32, 756

Craggs, J.D. and Meek, J.M. (1954), High Voltage Laboratory Technique, Butterworths' Scientific Publications, p. 179

Golovin, I.M. et al (1958), Proc. of the II U.N. Int. Conf. on the Peaceful Uses of Atomic Energy, 32, 72

Lovberg, R.H. (1959), Ann. Phys. 8, 311

Segre, S.E. and Allen, J.E. (1960), J. of Sci. Inst. 37, 369

Theophanis, G.A. (1960), Rev. Sci. Inst. 31, 427